

**FIRST AND SECOND LAW ANALYSES
OF
A BIOMASS FUELLED SOLID OXIDE FUEL CELL – MICRO TURBINE
HYBRID SYSTEM**

**A THESIS SUBMITTED TO
THE GRADUATE SCHOOL OF NATURAL AND APPLIED SCIENCES
OF
MIDDLE EAST TECHNICAL UNIVERSITY**

BY

SELİN ARABACI

**IN PARTIAL FULFILLMENT OF THE REQUIREMENTS
FOR
THE DEGREE OF MASTER OF SCIENCE
IN
MECHANICAL ENGINEERING**

NOVEMBER 2008

Approval of the thesis:

“FIRST AND SECOND LAW ANALYSES OF A BOMASS FUELLED SOLID
OXIDE FUEL CELL – MICRO TURBINE HYBRID SYSTEM”

submitted by **SELİN ARABACI** in partial fulfillment of the requirements for the
degree of **Master of Science in Mechanical Engineering, Middle East Technical
University** by,

Prof. Dr. Canan ÖZGEN
Dean, Graduate School of **Natural and Applied Sciences** _____

Prof. Dr. Süha ORAL
Head of the Department, **Mechanical Engineering** _____

Prof. Dr. Hafit YÜNCÜ
Supervisor, **Mechanical Engineering Dept., METU** _____

Examining Committee Members:

Assoc. Prof. Dr. Cemil YAMALI
Mechanical Engineering Dept., METU _____

Prof. Dr. Hafit YÜNCÜ
Mechanical Engineering Dept., METU _____

Prof. Dr. Abdullah ULAŞ
Mechanical Engineering Dept., METU _____

Prof. Dr. Tülay YEŞİN
Mechanical Engineering Dept., METU _____

Assoc. Prof. Dr. Atilla BIYIKOĞLU
Mechanical Engineering Dept., Gazi University _____

Date: _____

I hereby declare that all information in this document has been obtained and presented in accordance with academic rules and ethical conduct. I also declare that, as required by these rules and conduct, I have fully cited and referenced all material and results that are not original to this work.

Name, Last Name: Selin ARABACI

Signature:

ABSTRACT

FIRST AND SECOND LAW ANALYSES OF A BIOMASS FUELLED SOLID OXIDE FUEL CELL – MICRO TURBINE HYBRID SYSTEM

Arabacı, Selin

M.S. Department of Mechanical Engineering

Supervisor: Prof. Dr. Hafit Yüncü

November 2008, 75 pages

Fuel cells are direct energy conversion devices to generate electricity. They have the lowest emission level of all forms of electricity generation. Fuel cells require no combustion of the fuel. The thermal energy gained from fuel cells may be utilized in micro turbines (gas turbines).

In this work, first and second law analyses are performed on a hybrid system consisting of a solid oxide fuel cell (SOFC) combined with a micro turbine to be able to find an optimum point of pressure and corresponding mass ratio to gain maximum

work output. Also another system with same equipments only without a gas turbine is investigated to see the effects of gas turbine. The analyses are performed utilizing a code written in MATLAB for each of the equipments. Fuel used is biomass with a certain concentration. To be able to use biomass in a fuel cell-micro turbine hybrid cycle, it is gasified and converted into a certain calorific value gas, with the use of gasifiers. In this study fluidized bed gasifier is utilized since it has the advantage of good mixing and high heat transfer leading to a uniform bed condition. Desulphuration and gas filter units will be implemented in order to clean the producer gas before being used in hybrid system. For a certain percentage of the fuel that may pass through the fuel cell without being used, a combustor is utilized. Optimum point mass and pressure ratios for system are $M_R = 0.6411$ and $P_r = 8$. Gas turbine supplies more power and higher efficiency to the system.

There are different choices for fuel selection in hybrid systems. The reason why biomass is examined among these is that it decreases the depletion of energy carriers and reduces the environmental impact.

Keywords: Solid oxide fuel cell, micro turbine, exergy, biomass, hybrid system

ÖZ

BİYOKÜTLE İLE ÇALIŞAN KATI OKSİT YAKIT HÜCRESİ VE MİKROTÜRBİNDEN OLUŞAN MELEZ SİSTEMİN BİRİNCİ VE İKİNCİ KANUN ANALİZLERİ

Arabacı, Selin

Yüksek Lisans, Makine Mühendisliği Bölümü

Tez Danışmanı : Prof. Dr. Hafit Yüncü

Kasım 2008, 75 sayfa

Yakıt hücreleri elektrik üretmede kullanılan direkt enerji dönüşüm araçlarıdır. Var olan elektrik üretim yöntemleri arasında en düşük emisyon değerine sahiptirler. Yakıt hücreleri yakıtın yanmasına gerek duymaz. Yakıt hücrelerinden elde edilen ısı mikro türbinlerde (gaz türbinleri) kullanılabilir.

Bu çalışmada bir katı oksit yakıt hücresi ve bir mikro türbinden oluşan melez bir sistemin birinci ve ikinci kanun analizleri yapılmış ve sistemin maksimum güç

üretimi sağlayacağı basınç ve kütle oranı değerlerine sahip olan optimum noktası bulunmaya çalışılmıştır. Ayrıca aynı sistem gaz türbini çıkarılarak tekrar incelenmiş ve gaz türbinin sisteme katkısı görülmüştür. Analizler her donanım için MATLAB yazılımında oluşturulan program yardımıyla gerçekleştirilmiştir. Kullanılan yakıt belli bir konsantrasyona sahip biyokütledir. Yakıt hücresi ve mikro türbinden oluşan melez sistemlerde biyokütlenin kullanılabilmesi için biyokütlenin gazlaştırıcılar kullanılarak belli bir kalori değerine sahip gaz haline dönüştürülmesi gerekmektedir. Mevcut çalışmada, iyi karışım ve yüksek seviyede ısı transferi gerçekleştirilebilir avantajları dolayısıyla yeknesak koşullara sahip bir yatak sağlayan akışkan yatak yanma odası kullanılmıştır. Buna ek olarak, melez sistemde kullanılmadan önce gazlaştırma işlemi sonrası elde edilen gazın temizlenmesi için sisteme sülfürden arındırma üniteleri ve gaz filtreleri eklenmiştir. Yakıtın yakıt hücresinden yanmadan geçen miktarından faydalanabilmek için de yanma odası kullanılmıştır. Sistem için en uygun (optimum) kütle ve basınç oranları $M_R=0.6411$ ve $P_r=8$ 'dir. Gaz türbini sisteme fazladan güç ve yüksek verim sağlamaktadır.

Melez sistemlerde kullanılacak yakıt için birçok seçenek vardır. Bu yakıtlar arasından biyokütlenin seçilmesinin nedeni enerji taşıyıcılarının tüketimini ve çevreye verilen zararı azaltmasıdır.

Anahtar kelimeler: *Katı oksit yakıt hücresi, mikro türbin, ekserji, biyokütle, melez sistem*

To My Father Kemal ÇIYRAK
To My Mother Emel ÇIYRAK
To My Sister Pelin ÇIYRAK
To My Husband Mehmet Aytunç ARABACI

ACKNOWLEDGEMENTS

I would like to thank to my supervisor Prof. Dr. Hafit YÜNCÜ for his guidance and insight throughout the research.

I would like to thank to TÜBİTAK_BİDEB for their support throughout the research.

I express sincere thanks to my family for their support and faith in me, and for their understanding in every step of my education.

TABLE OF CONTENTS

PLAGIARISM.....	iii
ABSTRACT.....	iv
ÖZ.....	vi
ACKNOWLEDGEMENTS.....	ix
TABLE OF CONTENTS.....	x
LIST OF TABLES.....	xii
LIST OF FIGURES.....	xiii
LIST OF SYMBOLS.....	xv
CHAPTERS	
1. INTRODUCTION	1
1.1 System Definition	1
2. LITERATURE SURVEY	5
2.1 Hybrid Systems	5
2.2 Biomass Utilization.....	6
3. FIRST LAW ANALYSES.....	8
3.1 Dryer	8
3.2 Gasifier.....	9
3.2.1 Biomass Fuel (Hybrid Poplar)	10
3.3 Solid Oxide Fuel Cell (SOFC).....	12
3.3.1 Electrochemical Reactions and Cell Voltage in Fuel Cell.....	15
3.4 Combustor.....	22
3.5 Gas Turbine (GT).....	24
3.6 Heat Exchangers.....	25
4. SECOND LAW ANALYSES.....	28
4.1 Dryer	29
4.2 Gasifier.....	30

4.3	Solid Oxide Fuel Cell (SOFC)	31
4.4	Gas Turbine (GT).....	32
4.5	Heat Exchangers.....	33
5.	RESULTS AND DISCUSSION	35
5.1	First Law Analyses Results.....	35
5.2	Second Law Analyses Results	44
5.3	Optimum Point For System.....	51
6.	CONCLUSION	65
	REFERENCES.....	70

LIST OF TABLES

Table 3. 1 : Proximate and ultimate analysis of hybrid poplar [14].....	11
Table 3. 2: Different gas compositions for different mass ratios at gasifier outlet....	12
Table 3. 3 : Reversible cell potentials for different operating pressure and mass ratios	16
Table 3. 4 : Reversible cell efficiencies for different operating pressure and mass ratios.....	17
Table 3. 5 : Actual cell voltages for different operating pressure and mass ratios	19
Table 3. 6 : SOFC power outputs in kJ/kg biomass.....	20
Table 3. 7 : Voltage efficiency values for different pressure and mass ratios	22
Table 3. 8 : Overall electrical efficiency values for SOFC	22
Table 5. 1 : Energy, exergy and their normalized values for System 1 at $M_R=0.6411$ $P_r=8$	50

LIST OF FIGURES

Figure 1. 1 : System 1 Schematic	3
Figure 1. 2 : System 1 Schematic	4
Figure 3. 1 : SOFC Operating voltages vs pressure ratio.....	20
Figure 3. 2 : SOFC Operating voltages vs mass ratio.....	21
Figure 4. 1: Dryer inlet and outlet flows	30
Figure 4. 2: SOFC inlet and outlet flows.....	32
Figure 5. 1 : First law efficiency of the system vs mass ratio	36
Figure 5. 2 : System electrical efficiency vs mass ratio.....	37
Figure 5. 3 : SOFC electrical efficiency vs mass ratio.....	37
Figure 5. 4 : SOFC first law efficiency vs mass ratio	38
Figure 5. 5 : System total power output vs mass ratio	39
Figure 5. 6 : SOFC power output vs pressure ratio.....	40
Figure 5. 7 : SOFC power output vs mass ratio	40
Figure 5. 8 : GT work vs mass ratio.....	42
Figure 5. 9 : SOFC required heat transfer vs mass ratio	43
Figure 5. 10 : Combustor required heat transfer vs mass ratio	43
Figure 5. 11 : Gasifier required heat transfer vs mass ratio	44
Figure 5. 12 : System second law efficiency vs mass ratio.....	45
Figure 5. 13 : System total irreversibility vs mass ratio.....	46
Figure 5. 14 : SOFC second law efficiency vs mass ratio	47
Figure 5. 15 : SOFC irreversibility vs mass ratio	47
Figure 5. 16 : Combustor irreversibility vs mass ratio.....	48
Figure 5. 17 : Gasifier irreversibility vs mass ratio.....	48
Figure 5. 18 : GT second law efficiency vs mass ratio	49
Figure 5. 19 : GT irreversibility vs mass ratio	50
Figure 5. 20 : Total system power output vs pressure ratio.....	52
Figure 5. 21 : System electrical efficiency vs pressure ratio.....	52

Figure 5. 22 : SOFC power output vs pressure ratio.....	53
Figure 5. 23 : SOFC electrical efficiency vs pressure ratio	54
Figure 5. 24 : GT power output vs pressure ratio	54
Figure 5. 25 : Total inlet heat transfer vs pressure ratio.....	55
Figure 5. 26 : System first law efficiency vs pressure ratio	56
Figure 5. 27 : SOFC required heat transfer vs pressure ratio.....	56
Figure 5. 28 : Combustor required heat transfer vs pressure ratio.....	57
Figure 5. 29 : Gasifier required heat transfer vs pressure ratio.....	58
Figure 5. 30 : System second law efficiency vs pressure ratio.....	58
Figure 5. 31: Exhaust temperature vs pressure ratio	59
Figure 5. 32 : Irreversibility of the system vs pressure ratio.....	60
Figure 5. 33 : SOFC second law efficiency vs pressure ratio.....	60
Figure 5. 34 : SOFC irreversibility vs pressure ratio.....	61
Figure 5. 35 : Combustor irreversibility vs pressure ratio	62
Figure 5. 36 : Gasifier irreversibility vs pressure ratio	63
Figure 5. 37 : GT second law efficiency vs pressure ratio.....	63
Figure 5. 38 : GT irreversibility vs pressure ratio	64

LIST OF SYMBOLS

Symbols

A	Area (m ²)
a	Specific exergy (kJ/kg)
\dot{A}^{ch}	Chemical exergy (kW)
\dot{A}^{th}	Thermomechanical exergy (kW)
C	Specific heat (kJ/kg.K)
E	Cell actual voltage (V)
E_o	Theoretical cell voltage (V)
E_r	Reversible cell voltage (V)
F	Faraday constant (= 96485 Coulomb/kmole)
h	Specific enthalpy (kJ/kg)
h_o	Specific enthalpy at restricted dead state (kJ/kg)
\dot{I}	Rate of irreversibility (kW)
i	Mean current density (A/m ²)
i_L	Limiting current density (A/m ²)
i_o	Exchange current density (A/m ²)
\dot{m}	Mass flow rate (kg/s)
\dot{m}_b	Biomass mass flow rate (kg/s)
M_R	Mass ratio (=air for fuel cell/air for system)
\dot{m}_{wb}	Mass flow rate of water in biomass (kg/s)
\dot{m}_{wv}	Mass flow rate of water vapor (kg/s)
n	Number of electrons
\dot{N}_i	Molar flow rate (kmole/s)
\dot{n}	Molar flow rate (kmole/s)

P	Pressure (atm) (kPa)
$P_{el,FC}$	Electrical power of fuel cell (kW)
P_o	Environment pressure (atm) (kPa)
P_r	Pressure ratio for gas turbine
\dot{Q}	Heat transfer rate (kW)
\dot{Q}_{max}	Maximum heat transfer rate (kW)
R	Universal gas constant (= 8.314 kJ/kg.K)
s_o	Specific entropy at restricted dead state (kJ/kg.K)
T	Temperature (K)
$T_{biomass}$	Biomass inlet temperature to the system (K)
T_o	Environment temperature (K)
U	Overall heat transfer coefficient (kW/m ² .K)
V_{act}	Activation polarization (V)
V_{con}	Concentration polarization (V)
V_{ohm}	Ohmic polarization (V)
\dot{W}	Power (kW)
x_i	Molar flow rate of species i
α	Transfer coefficient
β	Factor to find lower heating value of biomass
δ	Thickness (m)
$\Delta_f H_{T_o}^o (H_2O_{(g)})$	Enthalpy of formation of gaseous water at T_o (kJ)
ΔT_{lm}	Logarithmic mean temperature difference (K)
ϵ_{ch}	Specific chemical exergy (kJ/kg)
η_{conv}	Conversion efficiency
η_{elec}	Electrical efficiency
$\eta_{el,FC}$	Fuel cell electrical efficiency

η_{first}	First law efficiency
$(\eta_{II})_{system}$	System second law efficiency
η_{vol}	Voltage efficiency
μ_i^o	Restricted dead state chemical potential (kJ/kmole)
μ_{oi}	Chemical potential for environment (kJ/kmole)
ρ	Resistivity (Ωm)
φ^{ch}	Specific chemical exergy (kJ/kg)

Abbreviations

GT	Gas turbine
IRSOFC	Internal reforming solid oxide fuel cell
IGCC	Integrated gasification combined cycle
LHV	Lower heating value
SOFC	Solid oxide fuel cell
WWF	World Wild Fund for nature

CHAPTER 1

INTRODUCTION

1.1 System Definition

In this study, basically two systems are analyzed with a code written in MATLAB. System 1 (Fig. 1.1) consists of a solid oxide fuel cell (SOFC) and a bottoming micro turbine cycle with a gas turbine (GT), a compressor and a recuperator. System 2 (Fig. 1.2) consists of a SOFC with a bottoming heat exchanger instead of a micro turbine [1, 2, 3]. The fuel utilized in both systems is biomass wood (hybrid poplar) enters the dryer and dried to some extent and heated up to 100 °C. Then, it enters the gasifier to be decomposed into fuel gases with some air from the GT. The products of gasification consist of CO₂, CO, CH₄, H₂, O₂, N₂, SO₂, NO₂ and H₂O. With the help of the cyclone, the cycling of products is performed so the efficiency is increased. Passing through a heat exchanger, the gasification products enter the ceramic filter which is a high temperature available filter where ash and hazardous gases (NO₂ and SO₂) are removed. After the heat exchanger again, the products enter the anode side of the SOFC with the extra supplied water. On the other hand, air coming from the environment are taken into the compressor of GT and compressed. After being separated into two branches for both gasifier and fuel cell needs, the fuel cell feed enters the recuperator and heated as is done in the next heat exchanger. Then it enters the cathode of SOFC. The chemical reactions (reforming of CH₄, shifting of CO and the cell reaction of H₂) occur. The products consist of remaining CH₄ from reforming, remaining CO from shifting and remaining H₂ from the cell reaction with the unused N₂, O₂ and produced CO₂ and H₂O. These flows (anode and cathode outlets) enter the combustor after the heat exchanger. In the combustor, remaining CH₄, CO and H₂ are burned totally and the total products enter the turbine of GT to gain work in System 1. Since there is no GT in System 2 this mixture enters the heat

exchanger. Passing through and heating the compressor outlet in both systems, it performs a district heating of water and enters the dryer to perform the last duty for heating and drying of the biomass and exits the system. In literature, the systems shows higher efficiencies and net work outputs for System 1 which is hybrid, and in this study, this consideration will be investigated and effect of GT will be mentioned.

In the analyses, the temperature of the environment is taken to be $T_0 = 25^\circ \text{C}$, and pressure of the environment is $P_0 = 1 \text{ atm}$. The inlet air to the system from the compressor of the GT has a composition of 21 % O_2 and 79 % N_2 . The enthalpy and entropy of inlet air are calculated as the mixture property consisting of these two elements, O_2 and N_2 .

The standard molar chemical exergies of the species are taken from J. Szargut, D.R. Morris, and F.R. Steward, in which atmospheric pressure is $P_0=1.0 \text{ atm}$ [4].

The inlet temperature of the solid biomass is taken to be at T_0 . All the analyses results are found for 1 kg/s of biomass flowrate. All the species are assumed as ideal gases.

Basically two important parameters exist in the investigation of system analyses results. M_R ; which is the ratio of air flow rate separated for the fuel cell inlet at the outlet of compressor, to the air flow rate entering to the system (from the compressor) totally. The second one is the P_r ; the pressure ratio for the GT. Firstly, for each of P_r values, minimum possible M_R value is found according to the energy and exergy analyses results of the system and then the maximum M_R is found according to the minimum air amount of the gasification process. The minimum air amount for the gasifier means the maximum air amount for the fuel cell and cannot be larger than this value.

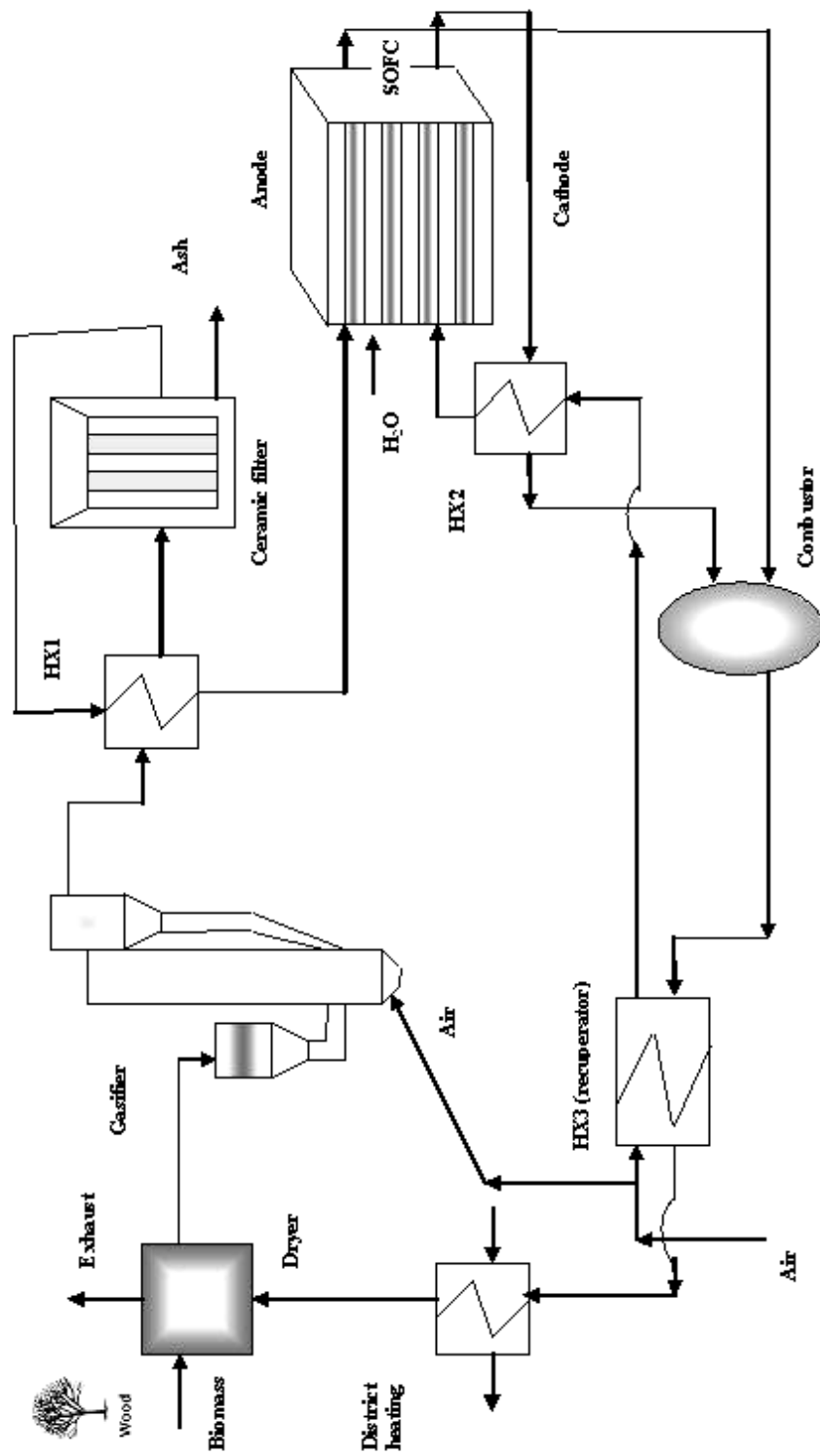


Figure 1. 2 : System 2 Schematic

CHAPTER 2

LITERATURE SURVEY

2.1 Hybrid Systems

Hybrid systems are mostly used to achieve much higher efficiencies than traditional GTs. As Uechi, Kimijima and Kasagi mentioned, the hybrid system consisting of a SOFC and a micro turbine is much superior to a recuperated GT in terms of its power generation efficiency and aptitude for small distributed generation. The best possible conceptual design of a 30-kW μ GT-SOFC hybrid system using methane as the fuel is shown to give power generation efficiency over 65 % (lower heating value (LHV) based) [1].

In study of Massardo, McDonald and Korakianitis, a 50-kW micro turbine coupled with a high-temperature SOFC. Natural gas is used as the fuel for the system and the system has a power output of 389 kW and an efficiency of 60 %. Utilizing the waste heat increases the overall fuel utilisation efficiency up to 80 %. 50-kW μ GT has a thermal efficiency of 29.5 % [2].

Freeh, Pratt and Brouwer studied about the modeling tools for aerospace applications of hybrid systems and compared the SOFC-GT hybrid system performance with experimental data. The electrochemical properties of fuel cell are considered at different operating pressures, temperatures and anode inlet compositions. The fuel utilized is kerosene-type jet fuel Jet-A for large commercial aircrafts. With this study they showed the improvement of fuel cell performance with pressure, change of cell resistance with temperature and effect of anode composition change on polarizations [3].

2.2 Biomass Utilization

Gasification is the basic step in biomass utilization in hybrid systems. McKendry studied the conversion of biomass by gasification. He found out that at the exit of gasification, CO, H₂ and CH₄ exist as products at different proportions which are dependent on use of air, oxygen or steam as the gasification medium with a concomitant range of calorific values between 4-40 MJ/Nm³. He mentioned that feedstock properties (moisture, ash, alkalis and volatiles) and feedstock pre-treatment (drying, particle size, fractionation and leaching) are important key parameters for gasification process. On economical aspect, he claimed that use of biomass from waste sources can influence the economics of plant operations in a positive manner and at the same time provide a means of assisting with the environmental problems posed by the disposal of wastes in the developed world [5].

Combined cycles with integrated biomass gasification is studied by Craig and Mann. They analyzed the cost and performance potential of three different biomass-based integrated gasification combined cycle (IGCC) systems. They chose high-pressure air-blown, low-pressure indirectly heated and low-pressure air-blown gasifiers. As a result, high pressure air-blown gasifier had the highest efficiency, the highest operating cost and the highest output power [6].

The advantages of circulating fluidized bed gasifier were analyzed and results were shown by Chen, Spliethoff, Andries and Glazer. Improved gasification is proposed. The biomass fuel utilized is miscanthus. The proposed gasification concept in the study could lead to maximum production rate of qualified product gas and also assure the compact configuration of gasifier and therefore appears advantageous and practical [7].

For biomass steam gasification in internal reforming SOFC (IRSOFC)-GT hybrid systems, Proell, Rauch, Aichernig and Hofbauer showed the performance of system

using the data of Guessing/Austria plant (8 MW fuel power). Electric efficiencies up to 40-43 %, gasifier chemical efficiency up to 72.4 % (LHV based for 20% water content) were found in simulations [8].

CHAPTER 3

FIRST LAW ANALYSES

3.1 Dryer

As explained in system definition, to gasify the biomass into fuels of SOFC (CO, CH₄ and H₂), it has to be dried to some acceptable extent to be reacted in the gasifier. The inlet and exit humidities of the biomass is taken as 35 % and 10 % (weight %) respectively [5, 6].

The mass balance for the dryer;

$$(\dot{m}_b)_{in} = (\dot{m}_b)_{out} \quad (3.1)$$

$$(\dot{m}_{wb})_{in} = (\dot{m}_{wb})_{out} + (\dot{m}_{wb})_v \quad (3.2)$$

where \dot{m}_b is the mass flow rate of dry biomass and stays constant throughout the dryer, $(\dot{m}_{wb})_{in}$ and $(\dot{m}_{wb})_{out}$ are the mass flowrates of water in biomass at the inlet and outlet of the dryer and $(\dot{m}_{wb})_v$ is the mass flow rate of water vaporized in dryer from the biomass.

The energy balance for the dryer;

$$\begin{aligned} \dot{m}_b \cdot ((h_b)_{in} - (h_b)_{out}) + (\dot{m}_{wb})_{in} \cdot ((h_w)_{in} - (h_w)_{out}) = & (\dot{m}_{wb})_{out} \cdot ((h_w)_{in} - (h_w)_{out}) \\ + (\dot{m}_{wb})_v \cdot ((h_w)_{in} - (h_w)_{out}) & \end{aligned} \quad (3.3)$$

$$\dot{m}_b \cdot ((h_b)_{in} - (h_b)_{out}) = \dot{m}_b \cdot C_b \cdot (T_o - (T_{out})_{dryer}) \quad (3.4)$$

The outlet is at $(T_{out})_{dryer} = 100^\circ\text{C}$ from the dryer inlet to the gasifier. The specific heat for the solid biomass is calculated from [9];

$$C_b = 1.125 + 0.00452 \cdot T \quad (3.5)$$

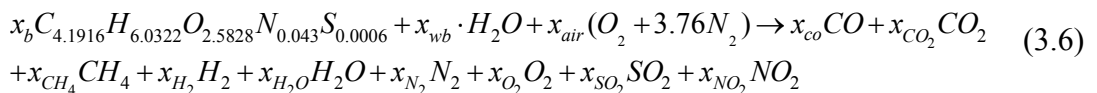
where T is in $^\circ\text{C}$ and C_b is in $\text{kJ/kg}\cdot^\circ\text{C}$. Here, C_b is constant and found at $T=25^\circ\text{C}$ as $1.238 \text{ kJ/kg}\cdot^\circ\text{C}$

3.2 Gasifier

Gasifier is used to decompose the biomass into CO , CH_4 and H_2 . For the incomplete oxidation of biomass, the chemical formula is taken to be $\text{C}_{4.1916}\text{H}_{6.0322}\text{O}_{2.5828}\text{N}_{0.043}\text{S}_{0.0006}$ for simplification. The inlet air to the gasifier comes from the compressor and the amount is between excess air of 0 to 50% [10]. The operating temperature of gasifier is $T_{\text{gasifier}} = 600^\circ\text{C}$.

The conversion ratio for the C in biomass at the exit of gasifier changes in literature according to the operating conditions and types of biomasses. However in this study this ratio is taken to be 6:3:1 for $\text{CO}:\text{CO}_2:\text{CH}_4$ [11, 12]. The output mixture of the gasifier mainly consists of CO , CO_2 , CH_4 , H_2 , H_2O , N_2 , O_2 and small amounts of NO_2 and SO_2 [7].

The chemical conversion in the gasifier can be shown as;



where x_i is the molar flow rate of each species i , for 1 kg/s of biomass flow rate according to the conversion ratios and air amounts given before.

Mass balance for the gasifier;

$$\dot{m}_b + \dot{m}_{wb} + (\dot{m}_{air})_{gas} = \dot{m}_{CO} + \dot{m}_{CO_2} + \dot{m}_{CH_4} + \dot{m}_{H_2} + \dot{m}_{H_2O} + \dot{m}_{N_2} + \dot{m}_{O_2} + \dot{m}_{SO_2} + \dot{m}_{NO_2} \quad (3.7)$$

where \dot{m}_{wb} is the mass flowrate of water in biomass and $(\dot{m}_{air})_{gas}$ is the mass flow rate of air inlet to the gasifier at exit temperature of compressor. The energy balance becomes;

$$\begin{aligned} \dot{m}_b \cdot (h_b)_{in} + \dot{m}_{wb} \cdot (h_w)_{in} + (\dot{m}_{air})_{gas} \cdot (h_{air})_{in} = \dot{m}_{CO} \cdot h_{CO} + \dot{m}_{CO_2} \cdot h_{CO_2} + \dot{m}_{CH_4} \cdot h_{CH_4} \\ + \dot{m}_{H_2} \cdot h_{H_2} + \dot{m}_{H_2O} \cdot h_{H_2O} + \dot{m}_{N_2} \cdot h_{N_2} + \dot{m}_{O_2} \cdot h_{O_2} + \dot{m}_{SO_2} \cdot h_{SO_2} + \dot{m}_{NO_2} \cdot h_{NO_2} + Q_{gasifier} \end{aligned} \quad (3.8)$$

where all the products are at $T_{gasifier}$. \dot{m}_i is the mass flow rate of each of the species i , where $()_{wb}$ stands for the water in the biomass and $()_b$ for dry biomass itself. $Q_{gasifier}$ is the heat transfer given out after the gasification reaction from the gasifier.

3.2.1 Biomass Fuel (Hybrid Poplar)

The ultimate and proximate analyses of the biomass are given in Table 3.1. The standard chemical exergy of the hybrid poplar, $(\varepsilon_{ch})_{biomass}$, is 19.2 MJ/kg [10]. The LHV can be calculated from Szargut and Styrylska [13];

$$(\varepsilon_{ch})_{biomass} = LHV_{biomass} \cdot \beta \quad (3.9)$$

where β is a factor that is calculated from the Equation 3.10;

Table 3. 1 : Proximate and ultimate analysis of hybrid poplar [14]

<u>Proximate Analysis (%dry fuel)</u>	
Fixed carbon	12.49
Volatile matter	84.81
Ash	2.70
<i>Total</i>	100.00
<u>Ultimate Analysis (%dry fuel)</u>	
Carbon	50.18
Hydrogen	6.06
Oxygen (diff.)	40.43
Nitrogen	0.60
Sulphur	0.02
Chlorine	0.01
Ash	2.70
<i>Total</i>	100.00

$$\beta = \frac{1.414 + 0.177 \cdot \left(\frac{H}{C}\right) - 0.3328 \cdot \left(\frac{O}{C}\right) \cdot \left(1 + 0.0537 \cdot \left(\frac{H}{C}\right)\right)}{1 - 0.4021 \cdot \left(\frac{O}{C}\right)} \quad (3.10)$$

for $0.5 < \frac{O}{C} \leq 2.0$. O, C and H are the mole fractions of oxygen, carbon and hydrogen in biomass fuel. For this study, the LHV is calculated as 16.46 MJ/kg for hybrid poplar.

One of the system parameters is M_R . Required air for gasifier and fuel cell is determined with this parameter. The maximum M_R occurs at minimum air amount for the gasification and maximum air amount for fuel cell. The total air amount inlet to the system from compressor is constant for all analyses cases. The minimum air amount for the gasifier is at 0 % excess air and the rest is the maximum air amount for the fuel cell which is twice the stoichiometric amount. For different M_R values, the gasifier outlet flow compositions in this study are given in Table 3.2.

Table 3. 2: Different gas compositions for different mass ratios at gasifier outlet

	<u>M_R=0.4539</u>	<u>M_R=0.4600</u>	<u>M_R=0.4665</u>	<u>M_R=0.5330</u>	<u>M_R=0.5871</u>	<u>M_R=0.6411</u>
<u>CO</u>	0.01634	0.01634	0.01634	0.01634	0.01634	0.01634
<u>CO₂</u>	0.00817	0.00817	0.00817	0.00817	0.00817	0.00817
<u>CH₄</u>	0.00272	0.00272	0.00272	0.00272	0.00272	0.00272
<u>H₂</u>	0.01415	0.01415	0.01415	0.01415	0.01415	0.01415
<u>H₂O</u>	0.00401	0.00401	0.00401	0.00401	0.00401	0.00401
<u>O₂</u>	0.01706	0.01678	0.01648	0.01338	0.01090	0.00839
<u>N₂</u>	0.09517	0.09410	0.09297	0.08131	0.07196	0.06254
<u>NO₂</u>	0.00028	0.00028	0.00028	0.00028	0.00028	0.00028
<u>SO₂</u>	0.00000	0.00000	0.00000	0.00000	0.00000	0.00000
<u>Total</u>	0.15791	0.15655	0.15513	0.14037	0.12854	0.11661

3.3 Solid Oxide Fuel Cell (SOFC)

For IRSOFCs, high operating temperatures allows internal steam reforming of methane and shifting of carbon monoxide at anode surface which guarantees high fuel conversion rates.

All hydrocarbons except methane should be removed from the producer gas because of the risk of carbon deposition on fuel electrode [8].

The electrochemical reaction taking place at the three-phase boundary fuel-anode-electrolyte is;



On cathode side oxygen is electrochemically reduced to oxygen ions, which are actually transported in electrolyte;

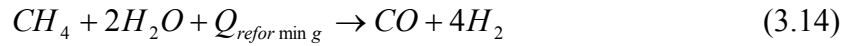


Overall oxidation reaction is therefore;



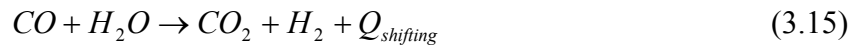
The fuel utilisation for the SOFC may change between 50-80% [8, 15]. In this study according to this range fuel utilisation is taken constant as 60%.

The anode is a well catalyst for steam reforming of CH₄, which is an endothermic reaction, according to;



This reforming reaction converts most of the CH₄ into CO and H₂ at operating conditions of SOFC [8]. The steam to methane ratio in literature is given in the range 2.2-3.0 [15]. From this information, in this study, 99% of methane is assumed to be reformed in fuel cell anode and the ratio of steam to methane is taken as 2.5.

At operating temperatures of SOFC, a direct electrochemical oxidation of CO at the anode-electrolyte boundary would be theoretically possible [8]. To avoid carbon deposition, steam to carbon ratio in the anode feed must be high enough, typically 2.0-3.5 [8,16,17]. In this study, according to this information, this steam to carbon ratio is taken to be 2.0. The shifting reaction in Equation 3.15, which is exothermic is assumed to occur at a percentage of 99.5% [16];



Mass balance for the SOFC becomes;

$$(\dot{m}_{an})_{in} + (\dot{m}_{cat})_{in} + \left((\dot{m}_{an})_{H_2O} \right)_{in} = (\dot{m}_{an})_{out} + (\dot{m}_{cat})_{out} \quad (3.16)$$

where anode inlet flow consists of the outlet total flow of gasifier except NO₂ and SO₂ which are removed from the flow in ceramic filter and cathode inlet flow consists of the air separated for the fuel cell in the compressor exit. $\left((\dot{m}_{an})_{H_2O} \right)_{in}$ stands for the inlet flow rate of steam into the anode side of the SOFC required for the reforming and shifting reactions. For the outlet flow rates, the anode side includes H₂O, CO₂, O₂ and N₂ that were already present in anode inlet coming from the gasifier outlet and CO, CH₄ and H₂ that are unburned in fuel cell reactions. The cathode side outlet flow includes O₂ that is not utilized in cell reaction and N₂ already present in incoming air.

The inlet flow of SOFC anode is at the exit temperature of first heat exchanger. The inlet of cathode is at cold side exit temperature of second heat exchanger. Both outlet flows of SOFC are at T_{SOFC} = 800°C.

For the energy balance of the SOFC;

$$\begin{aligned} & \dot{m}_{CO} \cdot h_{CO} + \dot{m}_{CO_2} \cdot h_{CO_2} + \dot{m}_{CH_4} \cdot h_{CH_4} + \dot{m}_{H_2} \cdot h_{H_2} + \dot{m}_{H_2O} \cdot h_{H_2O} + \dot{m}_{N_2} \cdot h_{N_2} + \dot{m}_{O_2} \cdot h_{O_2} \\ & + \left((\dot{m}_{O_2})_{cat} \right)_{in} \cdot h_{O_2} + \left((\dot{m}_{N_2})_{cat} \right)_{in} \cdot h_{N_2} + \dot{Q}_{FC} = \left((\dot{m}_{CO})_{an} \right)_{out} \cdot h_{CO} + \left((\dot{m}_{CO_2})_{an} \right)_{out} \cdot h_{CO_2} \quad (3.17) \\ & + \left((\dot{m}_{CH_4})_{an} \right)_{out} \cdot h_{CH_4} + \left((\dot{m}_{H_2})_{an} \right)_{out} \cdot h_{H_2} + \left((\dot{m}_{H_2O})_{an} \right)_{out} \cdot h_{H_2O} + \left((\dot{m}_{N_2})_{an} \right)_{out} \cdot h_{N_2} \\ & + \left((\dot{m}_{O_2})_{an} \right)_{out} \cdot h_{O_2} + \left((\dot{m}_{N_2})_{cat} \right)_{out} \cdot h_{N_2} + \left((\dot{m}_{O_2})_{cat} \right)_{out} \cdot h_{O_2} + \left((\dot{m}_{H_2O})_{react} \right)_{out} \cdot h_{H_2O} + \dot{W}_{FC} \end{aligned}$$

where subscript $\left(()_{an} \right)_{out}$ means anode side outlet, $\left(()_{cat} \right)_{out}$ means cathode side outlet and $\left(()_{react} \right)_{out}$ means product of cell reaction. \dot{Q}_{FC} and \dot{W}_{FC} are net inlet heat

transfer into the fuel cell and net electrical power produced in fuel cell reactions respectively.

The electrical power produced in the fuel cell, \dot{W}_{FC} can be found from the electrochemical reactions that are explained in Section 3.3.1.

3.3.1 Electrochemical Reactions and Cell Voltage in Fuel Cell

Overall electrical efficiency of the cell stack including DC/AC inverter is [8];

$$\eta_{el,FC} = \eta_r \cdot \eta_{vol} \cdot \eta_{conv} \cdot \eta_{inv} = \frac{P_{el,FC}}{\dot{m}_{a,in} \cdot LHV_{a,in}} \quad (3.18)$$

η_r is the reversible cell efficiency and is defined as;

$$\eta_r = \frac{E_r}{E_o} \quad (3.19)$$

where E_r is the reversible cell potential, also known as Nernst potential and E_o is the theoretical cell potential. Reversible cell efficiency in Equation 3.19 defines an upper bound for fuel cell efficiency comparable to Carnot efficiency for heat engines [8] .

E_r is the reversible cell potential given as [8];

$$E_r = \frac{-\Delta G^o_R(T)}{n \cdot F} + \frac{R \cdot T}{n \cdot F} \cdot \ln\left(\frac{P_{H_2} \cdot P_{O_2}^{1/2}}{P_{H_2O}}\right) \quad (3.20)$$

The open circuit voltage defined in Equation 3.20 depends on the T and partial pressures of gas species (P_{H_2} , P_{O_2} and P_{H_2O} are partial pressures of H₂, O₂ and H₂O respectively).

For this study, the reversible voltage results of SOFC for different operating pressure and mass ratios are given in Table 3.3.

E_o is the theoretical potential that corresponds to enthalpy of formation of gaseous H₂O at T_o and is a constant as [8];

$$E_o = \frac{-\Delta_f H_{T_o}^o (H_2O_{(g)})}{n \cdot F} = 1.253 \text{ V} \quad (3.21)$$

Then the reversible efficiencies defined in Equation 3.19 for this study are given in Table 3.4.

If current is drawn from fuel cell, voltage decreases with increasing current density due to irreversibility in fuel cell parts. This voltage drop is termed polarization or overvoltage. There are three types of polarizations basically; activation, ohmic and concentration polarizations.

Table 3. 3 : Reversible cell potentials for different operating pressure and mass ratios

	<u>P=1 atm</u>	<u>P=2 atm</u>	<u>P=4 atm</u>	<u>P=6 atm</u>	<u>P=8 atm</u>
<u>M_R = 0.6411</u>	0.885 V	0.901 V	0.917 V	0.926 V	0.933 V
<u>M_R = 0.5871</u>	0.887 V	0.903 V	0.919 V	0.928 V	-
<u>M_R = 0.5330</u>	0.889 V	0.905 V	0.921 V	0.931 V	-
<u>M_R = 0.4665</u>	0.892 V	0.908 V	0.924 V	-	-
<u>M_R = 0.4600</u>	0.893 V	0.909 V	-	-	-
<u>M_R = 0.4539</u>	0.893 V	-	-	-	-

Table 3. 4 : Reversible cell efficiencies for different operating pressure and mass ratios

	<u>P=1 atm</u>	<u>P=2 atm</u>	<u>P=4 atm</u>	<u>P=6 atm</u>	<u>P=8 atm</u>
<u>M_R = 0.6411</u>	0.706	0.719	0.732	0.739	0.745
<u>M_R = 0.5871</u>	0.708	0.721	0.733	0.741	-
<u>M_R = 0.5330</u>	0.709	0.723	0.735	0.743	-
<u>M_R = 0.4665</u>	0.712	0.725	0.737	-	-
<u>M_R = 0.4600</u>	0.712	0.725	-	-	-
<u>M_R = 0.4539</u>	0.713	-	-	-	-

Activation polarization can be derived from the Butler-Volmer equation as [8];

$$V_{act} = -2.3 \cdot \frac{R \cdot T}{\alpha \cdot n \cdot F} \cdot \log(i_o) + 2.3 \cdot \frac{R \cdot T}{\alpha \cdot n \cdot F} \cdot \log(i) \quad (3.22)$$

where i_o is the exchange current density in A/cm² which is the rate of oxidation or reduction of electrode at equilibrium expressed in terms of current. V_{act} is the activation polarization in volts and i is the mean current density of the cell stack in A/cm². The constants in front of the logarithmic terms are called Tafel constant and Tafel slope respectively [19]. R is the universal gas constant (=8.314 J/kg.K), T is the fuel cell temperature (=T_{SOFC}), α is the charge transfer coefficient (=0.5) [8], n is the number of moles of electrons per H₂ molecules (=2) and F is Faraday's constant (=96485 Coulomb/kmole). Exchange current density i_o is taken as 2000 A/m² at T_{SOFC}=1073 K [18].

Ohmic polarization occurs because of the resistance to flow of ions in the electrolyte and resistance to flow of electrons through the electrode materials. It is related to the resistivity and thickness of the materials used in the fuel cell [19]. The relation is;

$$V_{ohm} = i \cdot \sum_k \rho_k \cdot \delta_k \quad (3.23)$$

where ρ is the resistivity of the element k (anode, cathode, interconnect and electrolyte) δ is the thickness of each of these elements. i is the current density for the cell stack [8].

Concentration polarization is related to the decrease in reactant concentration at the surface of the electrodes as fuel is used. The relation is;

$$V_{con} = -\frac{R \cdot T}{n \cdot F} \cdot \ln\left(1 - \frac{i}{i_L}\right) \quad (3.24)$$

where i_L is the maximum (limiting) current density found from;

$$i_L(T) = a_{i_L} + b_{i_L} \cdot T \quad (3.25)$$

and for this study at operating conditions of SOFC, $a_{i_L} = 1750 \text{ A/m}^2$ and $b_{i_L} = 5.65 \text{ A/m}^2 \cdot \text{K}$ [8]. At limiting current density, the concentration at the catalyst surface is practically zero as the reactants are consumed as soon as they are supplied to the surface. The limiting current density for this study calculated from Equation 3.25 is $i_L(1073) = 7813 \text{ A/m}^2$.

The actual cell voltage at a certain current density is then;

$$E = E_r - V_{act} - V_{ohm} - V_{con} \quad (3.26)$$

For all the operating pressures and mass ratios of this study, the actual cell voltages are seen in Table 3.5.

Table 3. 5 : Actual cell voltages for different operating pressure and mass ratios

	<u>P=1 atm</u>	<u>P=2 atm</u>	<u>P=4 atm</u>	<u>P=6 atm</u>	<u>P=8 atm</u>
<u>M_R = 0.6411</u>	0.683 V	0.699 V	0.715 V	0.724 V	0.731 V
<u>M_R = 0.5871</u>	0.685 V	0.701 V	0.717 V	0.726 V	-
<u>M_R = 0.5330</u>	0.687 V	0.703 V	0.719 V	0.729 V	-
<u>M_R = 0.4665</u>	0.690 V	0.706 V	0.722 V	-	-
<u>M_R = 0.4600</u>	0.691 V	0.707 V	-	-	-
<u>M_R = 0.4539</u>	0.691 V	-	-	-	-

The activation, ohmic and concentration overpotentials for same amount of hydrogen (same current) in this study are calculated as;

$$V_{act} = 0.033 \text{ V} \quad V_{ohm} = 0.148 \text{ V} \quad V_{con} = 0.021 \text{ V}$$

Then fuel cell power output becomes;

$$\dot{W}_{FC} = E \cdot I \quad (3.27)$$

where E is the fuel cell operating voltage in volts and I is the current for fuel cell in A being $I = 2861 \text{ A}$ from the Equation 3.28 [20];

$$\left(\dot{n}_{H_2}\right)_{react} = \frac{i \cdot A}{n \cdot F} \quad (3.28)$$

where i is the current density in A/cm^2 , A is the total electrode area in the fuel cell (which is taken to be $100 \text{ cm}^2 \times 20000 \text{ cells}$), n is 2 for anode reaction and $\left(\dot{n}_{H_2}\right)_{react}$ is the number of moles of reacting hydrogen.

For this study the power outputs and operating voltage values for the fuel cell can be seen in Table 3.6 and also in Fig. 3.1 and 3.2.

Table 3. 6 : SOFC power outputs in kJ/kg biomass

	<u>P=1 atm</u>	<u>P=2 atm</u>	<u>P=4 atm</u>	<u>P=6 atm</u>	<u>P=8 atm</u>
<u>M_R = 0.6411</u>	1954.06	1999.84	2045.62	2071.36	2091.39
<u>M_R = 0.5871</u>	1959.79	2005.56	2051.34	2077.09	-
<u>M_R = 0.5330</u>	1965.51	2012.43	2057.06	2085.67	-
<u>M_R = 0.4665</u>	1974.09	2019.87	2065.64	-	-
<u>M_R = 0.4600</u>	1976.09	2022.73	-	-	-
<u>M_R = 0.4539</u>	1976.95	-	-	-	-

From the electrical efficiency definition of the cell in Equation 3.18, the voltage efficiency becomes;

$$\eta_{vol} = \frac{E}{E_r} \quad (3.29)$$

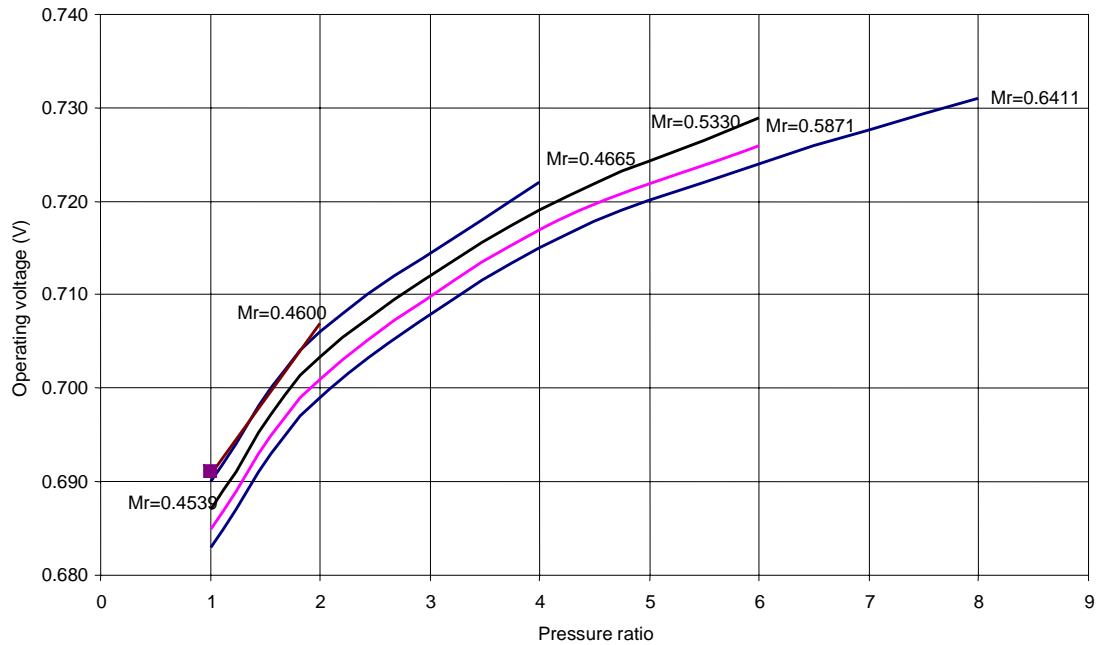


Figure 3. 1 : SOFC Operating voltages vs pressure ratio

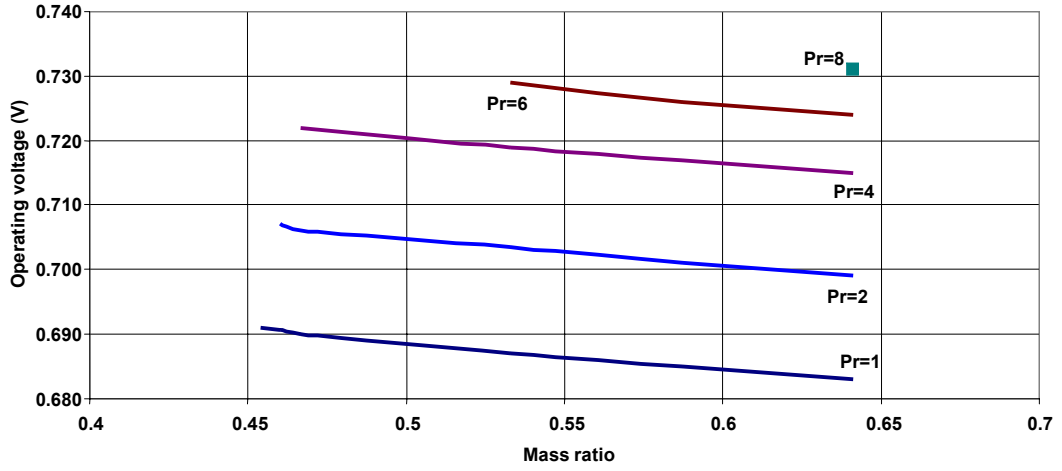


Figure 3. 2 : SOFC Operating voltages vs mass ratio

The voltage efficiency values for this study are given in Table 3.7.

In a real SOFC, the total fuel will never be completely converted into its components to produce power [8]. Therefore, the conversion efficiency of the cell stack can be generally defined as;

$$\eta_{conv} = \frac{(\dot{n}_{H_2})_{react} \cdot LHV_{H_2}}{(\dot{m}_a)_{in} \cdot (lhv_a)_{in}} \quad (3.30)$$

where $(\dot{n}_{H_2})_{react}$ is the amount of H_2 reacted in fuel cell; LHV_{H_2} and $(lhv_a)_{in}$ are the LHV of H_2 per mole and that of anode inlet flow and $(\dot{m}_a)_{in}$ is the anode inlet mass flow rate [8]. For this study for constant fuel and anode inlet flow rates, the conversion efficiency is calculated as 0.75.

The DC/AC inverter efficiency (η_{inv}) definition for the fuel cell in Equation 3.18 is taken as 96.5 % [8].

Table 3. 7 : Voltage efficiency values for different pressure and mass ratios

	<u>P=1 atm</u>	<u>P=2 atm</u>	<u>P=4 atm</u>	<u>P=6 atm</u>	<u>P=8 atm</u>
<u>M_R = 0.6411</u>	0.772	0.776	0.780	0.782	0.783
<u>M_R = 0.5871</u>	0.772	0.776	0.780	0.782	-
<u>M_R = 0.5330</u>	0.773	0.777	0.781	0.783	-
<u>M_R = 0.4665</u>	0.774	0.778	0.781	-	-
<u>M_R = 0.4600</u>	0.774	0.778	-	-	-
<u>M_R = 0.4539</u>	0.774	-	-	-	-

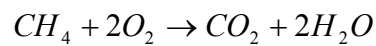
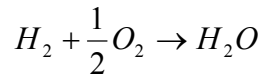
Table 3. 8 : Overall electrical efficiency values for SOFC

	<u>P=1 atm</u>	<u>P=2 atm</u>	<u>P=4 atm</u>	<u>P=6 atm</u>	<u>P=8 atm</u>
<u>M_R = 0.6411</u>	0.395	0.404	0.413	0.418	0.422
<u>M_R = 0.5871</u>	0.396	0.405	0.414	0.419	-
<u>M_R = 0.5330</u>	0.397	0.406	0.415	0.421	-
<u>M_R = 0.4665</u>	0.399	0.408	0.417	-	-
<u>M_R = 0.4600</u>	0.399	0.408	-	-	-
<u>M_R = 0.4539</u>	0.399	-	-	-	-

The overall electrical efficiencies for the fuel cell in this study are given in Table 3.8.

3.4 Combustor

All the unburned fuels at the exit of fuel cell anode is assumed to be burned in combustor [8,15]. The chemical reactions in the combustor are;



There is enough oxygen in the anode and cathode outlet flows for complete combustion so no extra air is required from outside into the combustor.

Mass balance for the combustor;

$$(\dot{m}_{an})_{out} + (\dot{m}_{cat})_{out} = \left((\dot{m}_{CO_2} + \dot{m}_{H_2O} + \dot{m}_{O_2} + \dot{m}_{N_2})_{comb} \right)_{out} \quad (3.32)$$

where \dot{m}_{CO_2} is the total CO₂ flow rate including product of fuel cell reactions and combustion reactions, \dot{m}_{H_2O} is the total H₂O flow rate including product of fuel cell reactions and combustion reactions, \dot{m}_{O_2} is the total O₂ flow rate showing total oxygen not utilized in combustor and \dot{m}_{N_2} is the total N₂ flow rate including all nitrogen at the outlets of fuel cell anode and cathode. $(\dot{m}_{an})_{out}$ is the total anode outlet flow rate including products of fuel cell reactions (CO₂, H₂O), oxygen and nitrogen coming from the gasifier (O₂, N₂) and unburned fuels (CO, CH₄ and H₂). $(\dot{m}_{cat})_{out}$ is the total air mass flowrate (nonutilized O₂ in fuel cell reactions and N₂ already existing in incoming air to the fuel cell). Then for the energy balance;

$$\begin{aligned} & \left(\left(\dot{m}_{CO} \cdot h_{CO} + \dot{m}_{CO_2} \cdot h_{CO_2} + \dot{m}_{CH_4} \cdot h_{CH_4} + \dot{m}_{H_2} \cdot h_{H_2} + \dot{m}_{H_2O} \cdot h_{H_2O} + \dot{m}_{N_2} \cdot h_{N_2} + \dot{m}_{O_2} \cdot h_{O_2} \right)_{an} \right)_{out} \\ & + \left(\left(\dot{m}_{N_2} \cdot h_{N_2} + \dot{m}_{O_2} \cdot h_{O_2} \right)_{cat} \right)_{out} = \left(\left(\dot{m}_{CO_2} \cdot h_{CO_2} + \dot{m}_{H_2O} \cdot h_{H_2O} + \dot{m}_{N_2} \cdot h_{N_2} + \dot{m}_{O_2} \cdot h_{O_2} \right)_{comb} \right)_{out} \\ & + \dot{Q}_{combustor} \end{aligned} \quad (3.33)$$

where the anode outlet is at T_{SOFC} and cathode outlet is at second heat exchanger hot fluid outlet temperature at the combustor inlet. All the exhaust from the combustor is at T_{combustor} = 750°C. $\dot{Q}_{combustor}$ is the total heat transfer rate given out from the combustor.

3.5 Gas Turbine (GT)

The micro turbine in System 1 consists of a compressor, a recuperator and a GT. Air for the whole system is compressed in compressor with $P_r = 2, 4, 6$ and 8 . Then it is separated into two branches being fuel cell and gasifier flows. The gasifier need is directly supplied to the gasifier and fuel cell need is sent to the recuperator. In the recuperator, it adiabatically exchanges heat with turbine outlet flow, which is the expanded form of combustor outlet in the GT. Then turbine flow from the recuperator goes to district heating and dryer whereas compressor flow goes to the second heat exchanger to adiabatically exchange heat with the cathode outlet flow of SOFC.

Mass balance for the compressor, turbine and recuperator are;

$$\dot{m}_{air} = (\dot{m}_{air})_{gas} + (\dot{m}_{cathode})_{in} \quad (3.34.a,b,c,d)$$

$$(\dot{m}_{comb})_{out} = (\dot{m}_{turb})_{out}$$

$$(\dot{m}_{cathode})_{in} = ((\dot{m}_{comp})_{rec})_{out}$$

$$(\dot{m}_{turb})_{out} = ((\dot{m}_{turb})_{rec})_{out}$$

where \dot{m}_{air} is the total air inlet to the system from the compressor; $(\dot{m}_{air})_{gas}$ is the air flow rate at the outlet of compressor going to the gasifier; $(\dot{m}_{cathode})_{in}$ is the air flow rate at the outlet of compressor going to the fuel cell cathode; $(\dot{m}_{comb})_{out}$ is the total exhaust flow rate from the combustor at the inlet of turbine; $(\dot{m}_{turb})_{out}$ is the flow rate of exhaust at the turbine outlet; $((\dot{m}_{turb})_{rec})_{out}$ and $((\dot{m}_{comp})_{rec})_{out}$ are the flow rates at the outlet of recuperator turbine flow outlet and compressor flow outlet.

The energy balance for the compressor, turbine and recuperator becomes;

$$\dot{m}_{air} \cdot h_{air} + \dot{W}_{comp} = (\dot{m}_{air})_{comp} \cdot (h_{air})_{comp} \quad (3.35.a, b,c)$$

$$(\dot{m}_{comb})_{out} \cdot (h_{comb})_{out} = (\dot{m}_{turb})_{out} \cdot (h_{turb})_{out} + \dot{W}_{turb}$$

$$\left((\dot{m}_{comp} \cdot h_{comp})_{rec} \right)_{out} - (\dot{m}_{air} \cdot h_{air})_{comp} = (\dot{m}_{turb} \cdot h_{turb})_{out} - \left((\dot{m}_{turb} \cdot h_{turb})_{rec} \right)_{out}$$

with isentropic efficiencies of compressor and turbine being 0.85 [3]. h_{air} is at T_o ; $(h_{comb})_{out}$ is at $T_{combustor}$; \dot{W}_{comp} and \dot{W}_{turb} are power required for compressor and power produced by the turbine respectively.

3.6 Heat Exchangers

Heat exchangers in both Systems 1 and 2 are analyzed by ϵ -NTU method since the outlet temperatures of the hot and cold fluids are unknown.

The maximum possible heat transfer rate is calculated from Equation 3.36;

$$\dot{Q}_{max} = (\dot{m} \cdot C_p)_{min} (T_{hi} - T_{ci}) \quad (3.36)$$

where T_{hi} and T_{ci} are inlet temperatures of hot and cold fluids respectively. $(\dot{m} \cdot C_p)_{min}$ is the minimum of hot and cold fluids heat capacities. Then using the effectiveness correlation in Equation 3.37 for counterflow heat exchangers corresponding effectiveness of the heat exchanger can be calculated[21];

$$\varepsilon = \frac{1 - \exp(-NTU \cdot (1 - C_r))}{1 - C_r \cdot (\exp(-NTU \cdot (1 - C_r)))} \quad C_r < 1 \quad (3.37)$$

where C_r is the ratio of minimum and maximum heat capacities of fluids, NTU is the number of transfer units calculated from Equation 3.38;

$$NTU = \frac{U \cdot A}{(\dot{m} \cdot C_p)_{\min}} \quad (3.38)$$

where U is the overall heat transfer coefficient and A is the area of heat exchangers taken from literature [22].

Heat transfer between the cold and hot fluids can be calculated from Equation 3.39;

$$\dot{Q} = \varepsilon \cdot (\dot{m} \cdot C_p)_{\min} \cdot (T_{hi} - T_{ci}) \quad (3.39)$$

Then outlet temperatures of cold and hot fluids can be calculated from Equations 3.40.a and 3.40.b;

$$T_{co} = T_{ci} + \frac{\dot{Q}}{(\dot{m} \cdot C_p)_c} \quad (3.40.a, b)$$

$$T_{ho} = T_{hi} - \frac{\dot{Q}}{(\dot{m} \cdot C_p)_h}$$

where T_{co} and T_{ho} are outlet temperatures of cold and hot fluids.

District heating part has known temperature values. Usable hot water inlet and exit temperatures are taken as 5°C and 85°C respectively [23]. The mass flow rate of

water in district heating is taken as 1 kg/s. According World Wild Fund for Nature (WWF) records, a person in Turkey uses 111 lt of water in one day [24]. 1 kg/s of water is enough for nearly 195 homes of four-people for one day.

CHAPTER 4

SECOND LAW ANALYSES

Exergy is defined as;

$$A = A^{th} + A^{ch} + E \quad (4.1)$$

where A^{th} is the thermo-mechanical flow exergy, A^{ch} is the chemical exergy and E is the sum of internal, kinetic and potential energies.

Exergy neglecting the kinetic and potential energies is;

$$A = (U - U_o) + P_o \cdot (V - V_o) - T_o \cdot (S - S_o) + \sum_{i=1}^n N_i \cdot (\mu_i^o - \mu_{oi}) \quad (4.2)$$

where A is the exergy, U is the internal energy, V is the volume, S is the entropy, N is the number of moles, and μ_{oi} is the chemical potential for environment. μ_i^o , U_o , P_o , V_o , T_o and S_o are restricted dead state properties.

The thermo-mechanical flow exergy is;

$$\dot{A}^{th} = \dot{m} \cdot ((h - h_o) - T_o \cdot (s - s_o)) \quad (4.3)$$

The chemical exergy is;

$$\dot{A}^{ch} = \sum_{i=1}^n \dot{N}_i \cdot (\mu_i^o - \mu_{oi}) \quad (4.4)$$

For a steady-state steady-flow process, if there is no chemical reaction in the device, then the exergy balance can be written as;

$$0 = \dot{W} - \dot{A}_e^{th} - \dot{A}_i^{th} + \dot{I} \quad (4.5)$$

where \dot{A}_i and \dot{A}_e are inlet and exit thermo-mechanical flow exergies and \dot{W} is actual work done by the system and \dot{I} is the rate of irreversibility.

4.1 Dryer

Dryer is a kind of heat exchanger. In this study, it is assumed to be adiabatic. Exergy balance applied for dryer is;

$$0 = \sum_e \dot{m}_e \cdot a_e^{th} - \sum_i \dot{m}_i \cdot a_i^{th} + \dot{I}_{dryer} \quad (4.6)$$

where a_i^{th} and a_e^{th} are specific thermo-mechanical flow exergies at inlet and exit of dryer. Inlet flows are the exhaust coming from the district heating and biomass inlet into the system (Fig. 4.1). Exhaust consists of CO₂, H₂O, O₂ and N₂. Biomass consists of dry biomass and water in itself.

Then, Equation 4.6 becomes;

$$\dot{I}_{dryer} = \left(\dot{m}_{CO_2} \cdot a_{CO_2}^{th} + \dot{m}_{H_2O} \cdot a_{H_2O}^{th} + \dot{m}_{O_2} \cdot a_{O_2}^{th} + \dot{m}_{N_2} \cdot a_{N_2}^{th} \right)_{distr} + \left(\dot{m}_b \cdot a_b^{th} + \dot{m}_{wb} \cdot a_{wb}^{th} \right)_{in} - \left(\dot{m}_{CO_2} \cdot a_{CO_2}^{th} + \dot{m}_{H_2O} \cdot a_{H_2O}^{th} + \dot{m}_{O_2} \cdot a_{O_2}^{th} + \dot{m}_{N_2} \cdot a_{N_2}^{th} \right)_{exh} - \left(\dot{m}_b \cdot a_b^{th} + \dot{m}_{wb} \cdot a_{wb}^{th} \right)_{out} \quad (4.7)$$

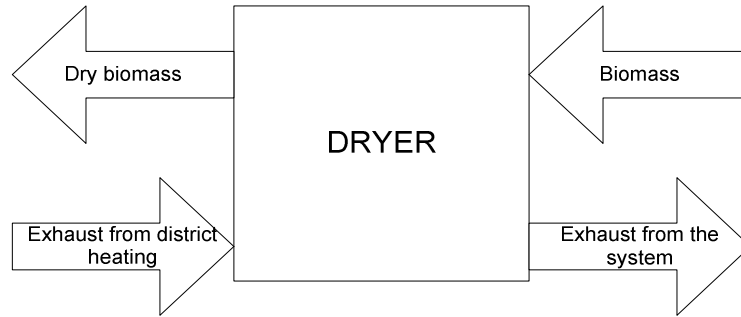


Figure 4. 1: Dryer inlet and outlet flows

where subscript *distr* shows the exit of district heating process (inlet to the dryer) and subscript *exh* is the exhaust from the system. Subscripts *in* and *out* shows the biomass with its water content at the inlet and exit of the dryer respectively. a^{th} is the specific thermomechanical flow exergy.

The specific thermo-mechanical flow exergy for the solid biomass at any temperature T can be found from;

$$a_b^{th} = C_b \cdot (T - T_o) - T_o \cdot C_b \cdot \ln\left(\frac{T}{T_o}\right) \quad (4.8)$$

where C_b is the specific heat of biomass.

4.2 Gasifier

For the gasification process, the chemical exergies should also be discussed in exergy balance. The chemical exergy values are tabulated in J. Szargut, D.R. Morris, and F.R. Steward [4]. When the exergy balance is rewritten for the gasifier;

$$\dot{I}_{gasifier} = \sum_i \dot{m}_i \cdot a_i - \sum_e \dot{m}_e \cdot a_e \quad (4.9)$$

where a is the total specific exergy including thermo-mechanical flow and chemical exergies and subscripts i and e denote the inlet and exit flows respectively.

Inlet flow for the gasifier consists of biomass and water in itself and air coming from the compressor of the GT whereas exit flow consists of CO, CO₂, H₂O, H₂, CH₄, O₂, N₂, NO₂ and SO₂. Then Equation 4.9 becomes;

$$\begin{aligned} \dot{I}_{gasifier} = & \left(\dot{m}_b \cdot a_b + \dot{m}_{wb} \cdot a_{wb} \right)_{gasbio} + \left(\dot{m}_{O_2} \cdot a_{O_2} + \dot{m}_{N_2} \cdot a_{N_2} \right)_{gasair} - \left(\dot{m}_{CO} \cdot a_{CO} + \dot{m}_{CO_2} \cdot a_{CO_2} \right. \\ & \left. + \dot{m}_{H_2O} \cdot a_{H_2O} + \dot{m}_{H_2} \cdot a_{H_2} + \dot{m}_{CH_4} \cdot a_{CH_4} + \dot{m}_{O_2} \cdot a_{O_2} + \dot{m}_{N_2} \cdot a_{N_2} + \dot{m}_{NO_2} \cdot a_{NO_2} + \dot{m}_{SO_2} \cdot a_{SO_2} \right)_{gasout} \end{aligned} \quad (4.10)$$

where $()_{gasair}$ shows the oxygen and nitrogen in inlet air coming from compressor to the gasifier and $()_{gasbio}$ shows the biomass with its water content at the inlet of gasifier. $()_{gasout}$ means the outlet section of gasifier.

4.3 Solid Oxide Fuel Cell (SOFC)

Electrochemical reactions take place inside the fuel cell. Therefore, chemical exergies should be involved with thermo-mechanical flow exergies as in the gasifier.

$$\begin{aligned} \dot{I}_{FC} = & \left(\left(\dot{m}_{CO} \cdot a_{CO} + \dot{m}_{CO_2} \cdot a_{CO_2} + \dot{m}_{H_2O} \cdot a_{H_2O} + \dot{m}_{H_2} \cdot a_{H_2} + \dot{m}_{CH_4} \cdot a_{CH_4} + \dot{m}_{O_2} \cdot a_{O_2} + \dot{m}_{N_2} \cdot a_{N_2} \right)_{an} \right)_{gasin} \\ & + \left(\dot{m}_{O_2} \cdot a_{O_2} + \dot{m}_{N_2} \cdot a_{N_2} \right)_{FCair} + \left(\left(\dot{m}_{H_2O} \cdot a_{H_2O} \right)_{an} \right)_{in} \\ & - \left(\left(\dot{m}_{CO} \cdot a_{CO} + \dot{m}_{CO_2} \cdot a_{CO_2} + \dot{m}_{H_2O} \cdot a_{H_2O} + \dot{m}_{H_2} \cdot a_{H_2} + \dot{m}_{CH_4} \cdot a_{CH_4} + \dot{m}_{O_2} \cdot a_{O_2} + \dot{m}_{N_2} \cdot a_{N_2} \right)_{an} \right)_{out} \\ & - \left(\left(\dot{m}_{O_2} \cdot a_{O_2} + \dot{m}_{N_2} \cdot a_{N_2} \right)_{cat} \right)_{out} - \dot{W}_{FC} \end{aligned} \quad (4.11)$$

where anode and cathode outlet flows are at T_{SOFC} , air inlet flow to SOFC shown with $()_{FCair}$ is at cold flow outlet temperature of second heat exchanger and anode inlet flow (shown with $(()_{an})_{gasin}$) is at cold side outlet temperature of first heat exchanger. Water inlet to SOFC is at $100^{\circ}C$ (shown with $(()_{an})_{in}$). Inlet and outlet flows for fuel cell can be seen in Fig. 4.2.

4.4 Gas Turbine (GT)

For the GT, each of turbine, compressor and recuperator are investigated separately. There is no chemical reaction occurring in none of these three equipments. For the compressor, considering the thermo-mechanical flow exergies, work is done on the system so;

$$\dot{I}_{comp} = \dot{m}_{air} \cdot a^{th}_{air} - (\dot{m}_{air} \cdot a^{th}_{air})_{comp} + \dot{W}_{comp} \quad (4.12)$$

$()_{comp}$ is used for compressed air at the exit.

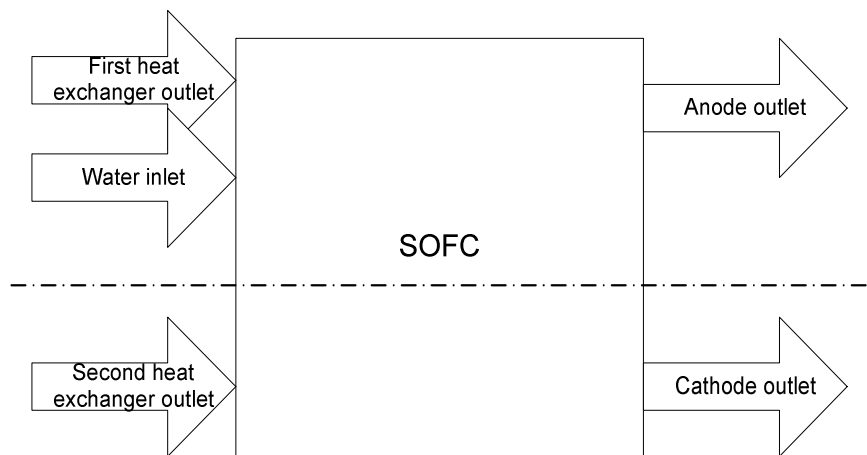


Figure 4. 2: SOFC inlet and outlet flows

For the turbine, work is done by the system so;

$$\dot{I}_{turb} = \left(\dot{m}_{comb} \cdot a^{th}_{comb} \right)_{out} - \left(\dot{m}_{turb} \cdot a^{th}_{turb} \right)_{out} - \dot{W}_{turb} \quad (4.13)$$

where $\left(()_{comb} \right)_{out}$ stands for combustor outlet flow (which is the inlet of turbine) and $\left(()_{turb} \right)_{out}$ stands for turbine outlet flow.

For the recuperator, similar to dryer;

$$\begin{aligned} \dot{I}_{rec} = & \left(\left(\dot{m}_{air} \cdot a^{th}_{air} \right)_{comp} + \left(\dot{m}_{turb} \cdot a^{th}_{turb} \right)_{out} \right)_{inlet} \\ & - \left(\left(\dot{m}_{comp} \cdot a^{th}_{comp} \right)_{rec} \right)_{out} + \left(\left(\dot{m}_{turb} \cdot a^{th}_{turb} \right)_{rec} \right)_{out} \end{aligned} \quad (4.14)$$

$()_{inlet}$ shows inlet to the recuperator, and $()_{outlet}$ shows outlet from the recuperator.

Total rate of irreversibility for the GT is then;

$$\dot{I}_{GT} = \dot{I}_{turb} + \dot{I}_{comp} + \dot{I}_{rec} \quad (4.16)$$

4.5 Heat Exchangers

For the heat exchangers, exergy balance equations are applied on hot and cold fluids as;

$$0 = \sum_e \dot{m}_e \cdot a^{th}_e - \sum_i \dot{m}_i \cdot a^{th}_i + \dot{I}_{he} \quad (4.15)$$

where subscripts i and e shows inlet and exit of both hot and cold fluids respectively and \dot{I}_{he} is the rate of irreversibility for heat exchanger.

CHAPTER 5

RESULTS AND DISCUSSION

System 1 and System 2 are working at different mass and pressure ratios. System 1 has its minimum possible mass and pressure ratio as $M_R=0.4600$ at $P_r=2$. System 2 has its minimum possible mass ratio as $M_R=0.4539$. Since there is no gas turbine there is no other possible pressure ratio for System 2. For both System 1 and System 2, the maximum mass ratio is $M_R=0.6411$ and possible maximum pressure ratio for System 1 is $P_r=8$. This operating range is calculated from the energy and exergy balances.

5.1 First Law Analyses Results

First law analyses of the two systems are investigated in terms of heat transfers, power outputs and efficiencies. The first law efficiency considering the system as a cycling heat engine is defined as;

$$\eta_{first} = \frac{\dot{W}_{system}}{\left(\dot{Q}_{system}\right)_{in}} \quad (5.1)$$

where \dot{W}_{system} is the total power output of the system and $\left(\dot{Q}_{system}\right)_{in}$ is the total inlet heat transfer to the system. The results are given in Fig. 5.1.

When Fig. 5.1 is examined, maximum first law efficiency is at $P_r = 8$ and $M_R = 0.6411$. At constant pressure ratio line, the first law efficiency increases with increasing mass ratio, which means increasing air amount into the fuel cell.

Therefore, without changing the total air inlet amount to the system, increasing the air inlet to the SOFC increases the first law efficiency of the system.

Electrical efficiency for the system is defined as [8];

$$\eta_{elec} = \frac{\dot{W}_{system}}{\dot{m}_{fuel} \cdot LHV_{fuel}} \quad (5.2)$$

This efficiency definition shows the ratio of total work output of the system to the LHV of fuel. Results of calculation of system electrical efficiency are given in Fig. 5.2.

In Fig.5.2, the maximum electrical efficiency is at $P_r=8$ and $M_R = 0.6411$. At constant pressure ratio line, increasing the mass ratio which means increasing the air amount inlet to the SOFC, does not change the electrical efficiency of the system.

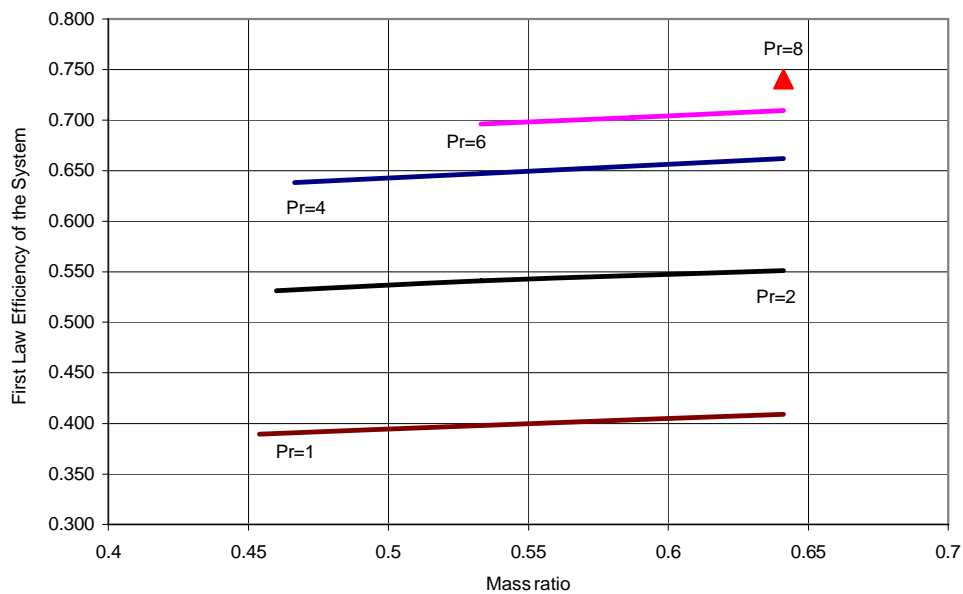


Figure 5. 1 : First law efficiency of the system vs mass ratio

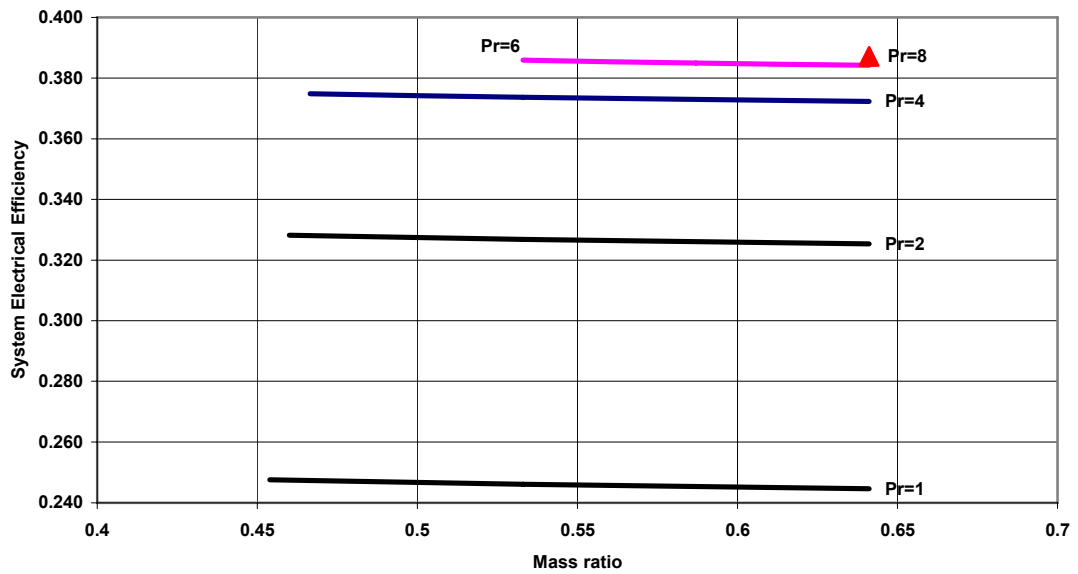


Figure 5. 2 : System electrical efficiency vs mass ratio

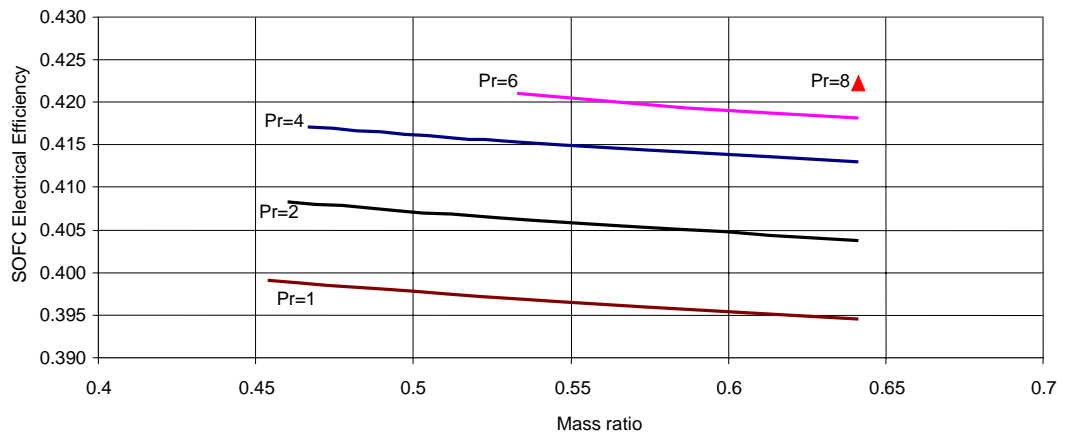


Figure 5. 3 : SOFC electrical efficiency vs mass ratio

SOFC electrical efficiency was defined in Section 3.3.1. Electrical efficiency for fuel cell includes reversible cell efficiency, voltage efficiency, conversion efficiency and

inverter efficiency as defined in Equation 3.18. The effects of pressure ratio and mass ratio on electrical efficiency of SOFC are given in Fig. 5.3.

Maximum electrical efficiency for SOFC is at $P=8$ atm. Increase of pressure increases the electrical efficiency of the SOFC at constant mass ratio. Increase in the mass ratio at constant pressure line decreases the electrical efficiency of the SOFC.

Fig. 5.4 shows the results of first law efficiency calculation of SOFC. The definition of first law efficiency for a system is given in Equation 5.1. For SOFC, the same definition is valid. Maximum first law efficiency for SOFC is at $P_r=4$ and $M_R=0.4665$. Increasing the mass ratio at constant pressure ratio line, decreases the first law efficiency of the SOFC.

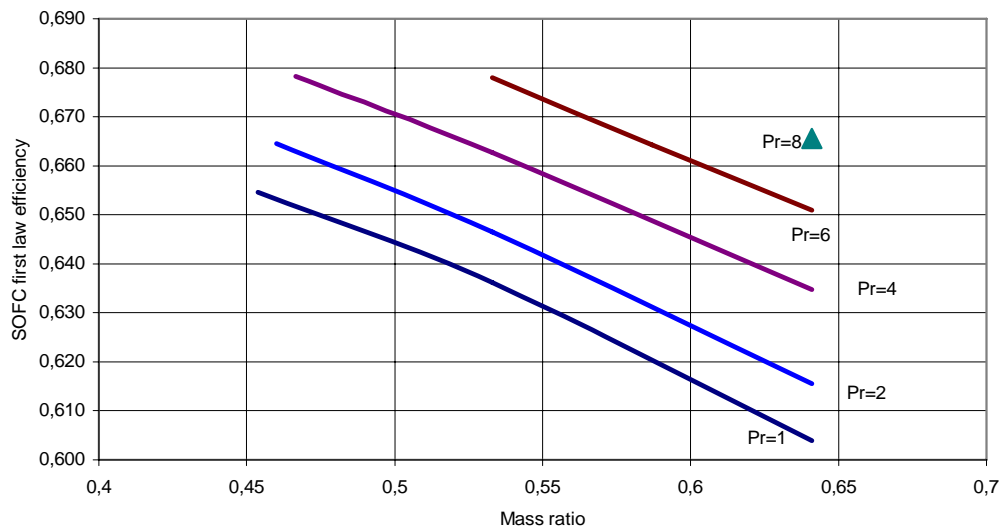


Figure 5. 4 : SOFC first law efficiency vs mass ratio

Total system work output is given in Fig. 5.5. Maximum work output is at $P_r=8$, $M_R=0.6411$. System electrical efficiency was also the highest at this point for same amount of fuel in Fig. 5.2. System 1 includes a GT so higher power output is as predicted when compared to System 2 results. As can be seen from the figure, $P_r=1$ is System 1 work output line and it has the minimum work output.

When change of mass ratio is considered, at constant pressure ratio line, as the mass ratio increases, the total power output of the system does not change.

For SOFC and GT, the power output figures are given in Fig. 5.6, 5.7 and 5.8 respectively. SOFC power output has its maxima at $P_r=8$ $M_R=0.6411$. Mass ratio increase leads to decrease in power output of fuel cell for same amount of reacting fuel at constant pressure line. Increasing the air amount inlet to the SOFC, decreases the air inlet to the gasifier since the total air inlet to the system is kept constant.

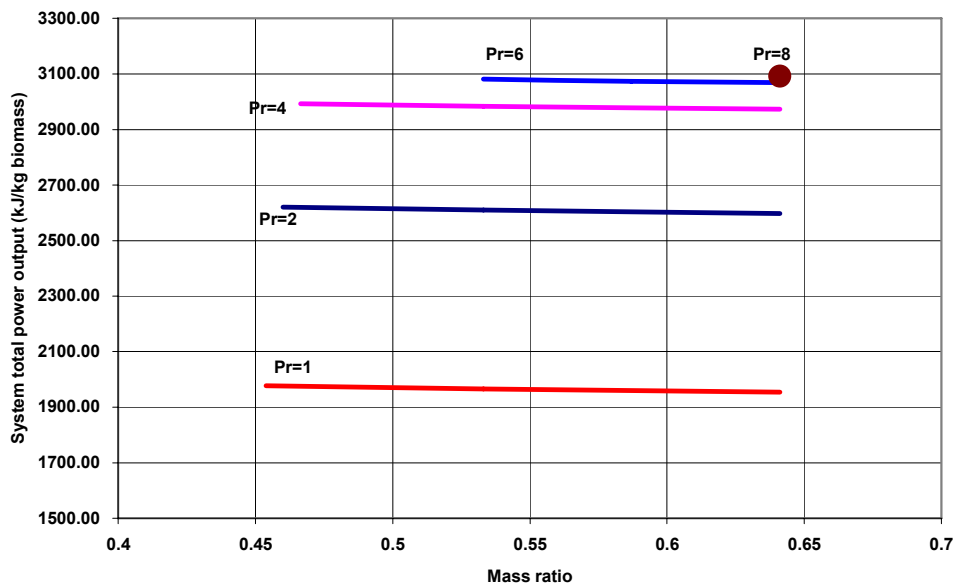


Figure 5. 5 : System total power output vs mass ratio

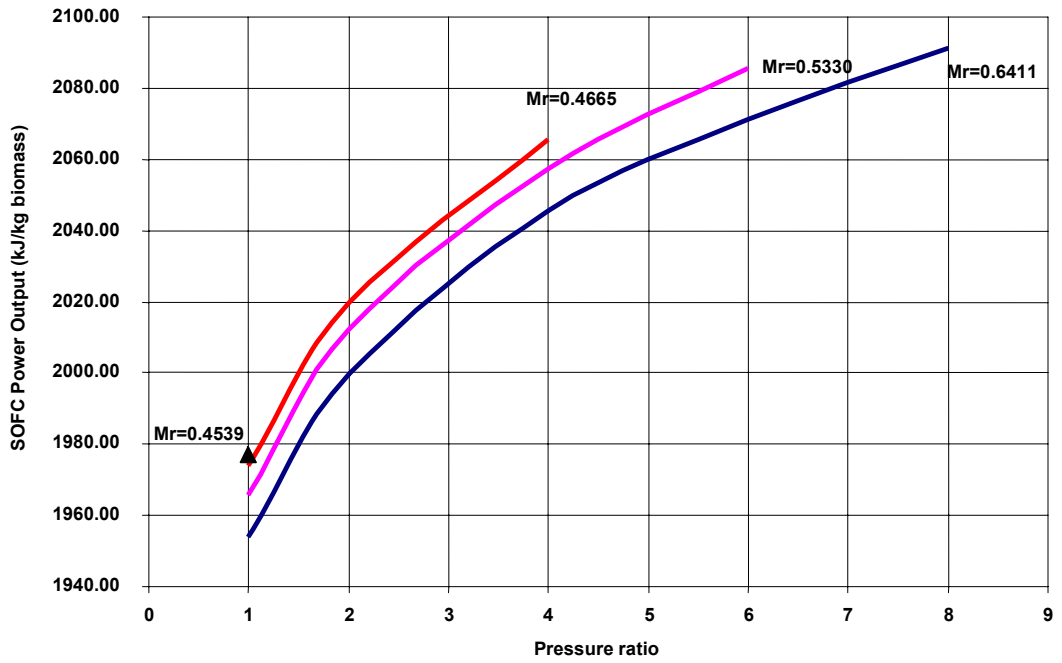


Figure 5. 6 : SOFC power output vs pressure ratio

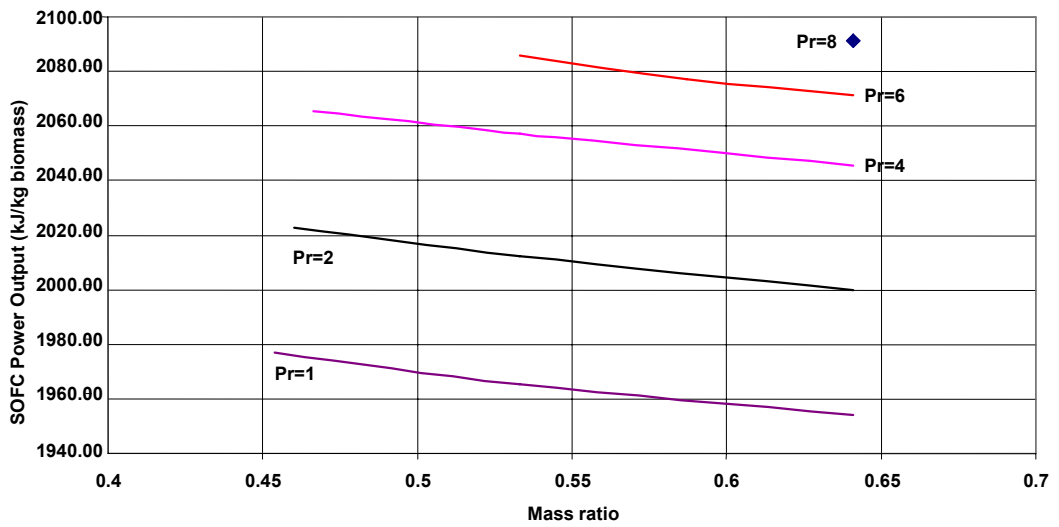


Figure 5. 7 : SOFC power output vs mass ratio

Then the amount of gases outlet from the gasifier decreases as in Table 3.2. Inlet gas amount into the SOFC anode decreases. Reacting H_2 amount does not change based on the assumption of constant fuel inlet to the system and constant fuel utilization in SOFC. This increases the partial pressure of fuel H_2 in anode side. The product H_2O partial pressure increases in same amount in anode with increasing mass ratio. Since reacting O_2 amount in cathode side of SOFC also does not change, increasing the mass ratio decreases the partial pressure of reacting O_2 . Decrease in partial pressure of reacting O_2 decreases the reversible cell potential of SOFC from Equation 3.20. Since polarization amount does not change because of constant operating current density assumption, actual cell voltage decreases. Therefore, power output decreases from Equation 3.27.

For pressure change in SOFC, it can be said that, at constant mass ratio, increase in pressure increases the partial pressure of O_2 which causes an increase in reversible cell potential and for constant polarization voltage, an increase in actual cell voltage. From Equation 3.27, the power output increases.

GT power output results are only available for System 1 as given in Fig. 5.8. Maximum power output for the GT is at $P_r = 8$, $M_R = 0.6411$. As the mass ratio increases, at constant pressure ratio line, air inlet to SOFC increases. This increases the outlet flow rate of SOFC cathode. However, SOFC anode outlet flow rate decreases because of the gasifier air inlet decrease. At the end, the inlet and exit flow rates to compressor and turbine does not change. This means mass ratio does not have any effect on GT work output.

For the first law analysis, heat transfer values should also be considered. SOFC, combustor and gasifier inlet heat transfer values can be seen in Fig. 5.9, 5.10 and 5.11 respectively.

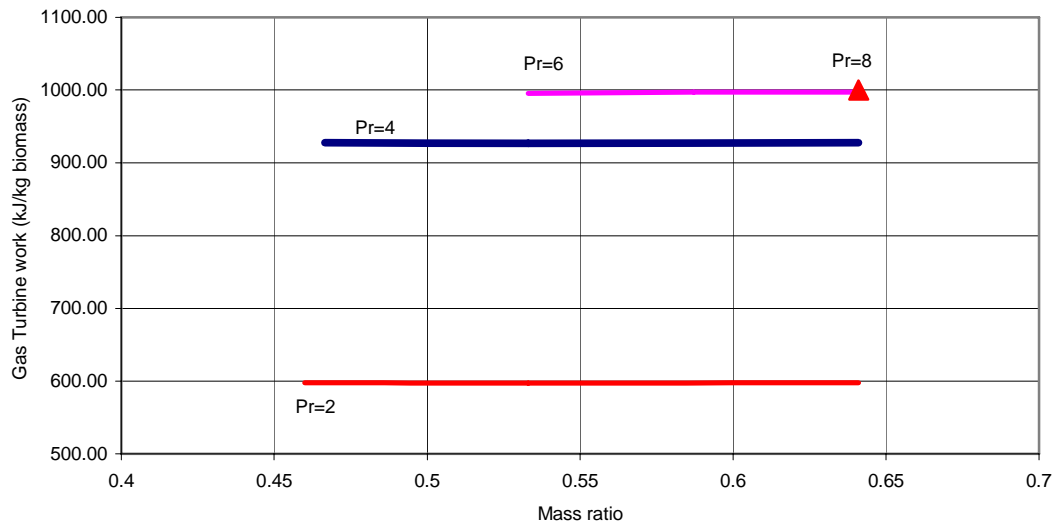


Figure 5. 8 : GT work vs mass ratio

For fuel cell in Fig. 5.9, required heat transfer does not change considerably with pressure since the species are all assumed to be ideal gases. However, mass ratio increase causes an increase in heat input rate. Increase in mass ratio decreases the outlet temperature of second heat exchanger flow inlet to the SOFC cathode. Since outlet temperatures of SOFC anode and cathode flows are the same for all cases being T_{SOFC} and inlet temperature of anode from first heat exchanger does not change considerably, this is the reason for increase in heat input to SOFC.

In Fig. 5.10, combustor gives out heat and this amount increases with increasing mass ratio and pressure. The maxima is at $P_r=8$ and $M_R=0.6411$. When the results are investigated, it is observed that the outlet enthalpy of combustor does not change since the outlet temperature is assumed to be constant in all cases as $T_{combustor}$. However, when the mass ratio increases, the inlet enthalpy decreases. Therefore, the inlet heat transfer to the combustor increases with increasing mass ratio. Same consideration applies for increasing pressure ratio.

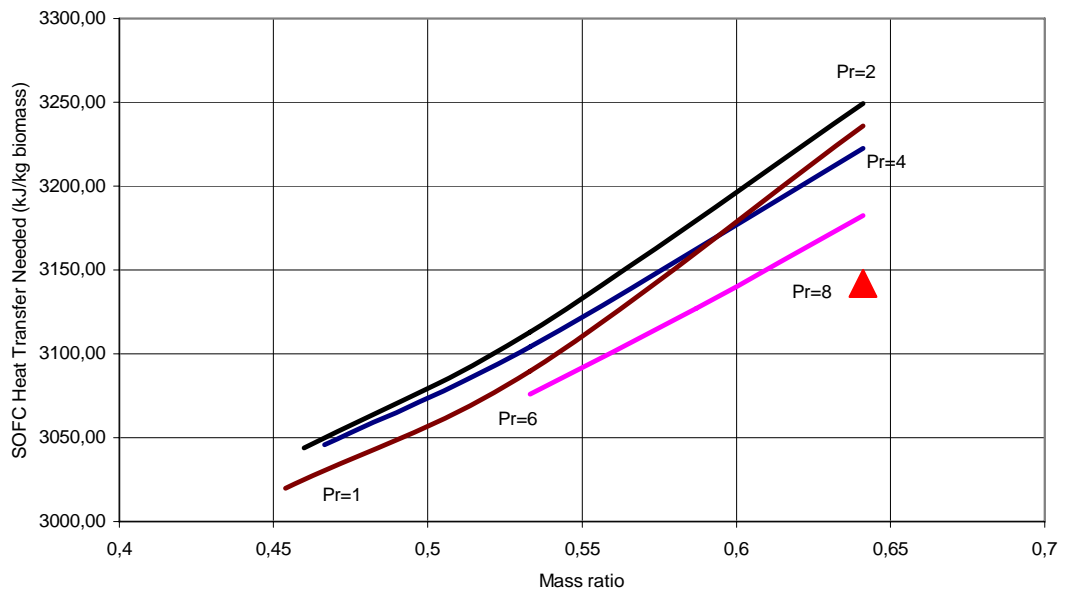


Figure 5. 9 : SOFC required heat transfer vs mass ratio

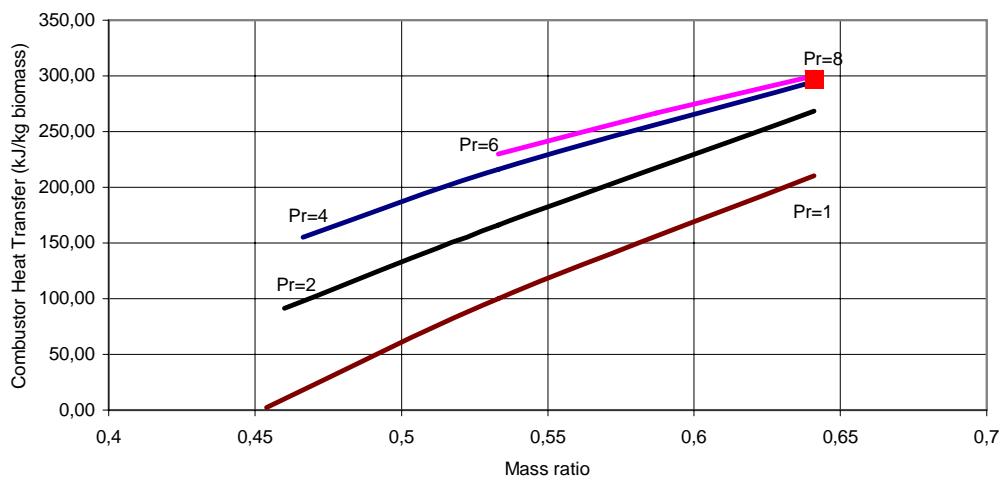


Figure 5. 10 : Combustor required heat transfer vs mass ratio

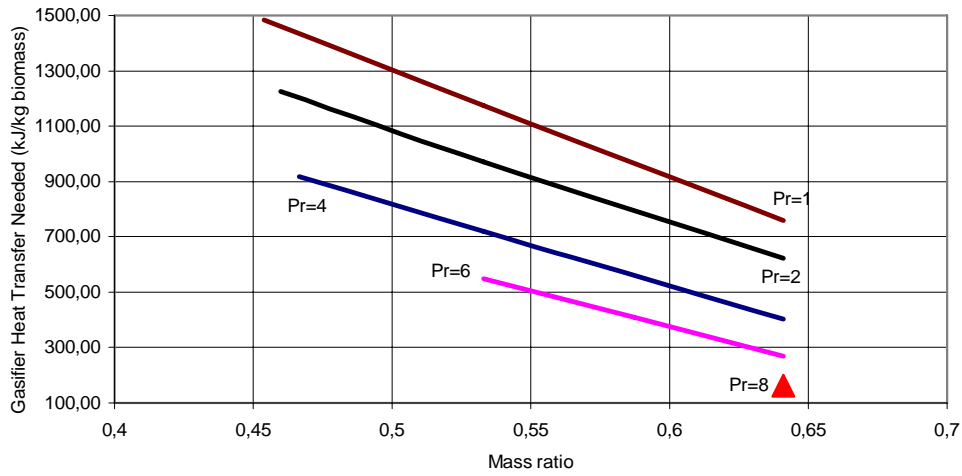


Figure 5. 11 : Gasifier required heat transfer vs mass ratio

In Fig. 5.11, gasifier has its minimum required heat input at $M_R = 0.6411$ at $P_r=8$. Since the inlet temperature and amount of biomass into the gasifier and outlet flow temperature do not change, the inlet air amount and temperature is important in input heat rate to the gasifier. For constant pressure ratio line, as the mass ratio increases the air amount inlet to the gasifier decreases. This decreases the required heat input for gasifier. For constant mass ratio, as the pressure ratio increases the outlet temperature of compressor air increases, which decreases the required heat input to the gasifier.

5.2 Second Law Analyses Results

Second law efficiency is defined as;

$$(\eta_{II})_{system} = \frac{\dot{W}_{system}}{(\dot{A}_{in} - \dot{A}_{out})_{system}} \quad (5.3)$$

where \dot{A}_{in} and \dot{A}_{out} are total inlet and outlet exergies. This efficiency definition shows how much of exergy in the system is utilized. The second law efficiencies are given in Fig. 5.12.

In Fig. 5.12, system second law efficiency is maximum at System 1, $P_r=8$ and $M_R = 0.6411$. The inlet exergy to the system does not change for none of the cases. Therefore, the main point is the irreversibility and outlet exergy for the systems analyses. At maximum second law efficiency, the irreversibility should be minimum and/or outlet exergy and work output should be maximum. As given in Fig. 5.5, the maximum work output is at same point $P_r=8$ and $M_R = 0.6411$.

The irreversibility graph is given for all cases in Fig. 5.13. When considered together with the Fig. 5.12, for this study, at maximum second law efficiency, the total irreversibility is the minimum ($P_r = 8$ and $M_R = 0.6411$).

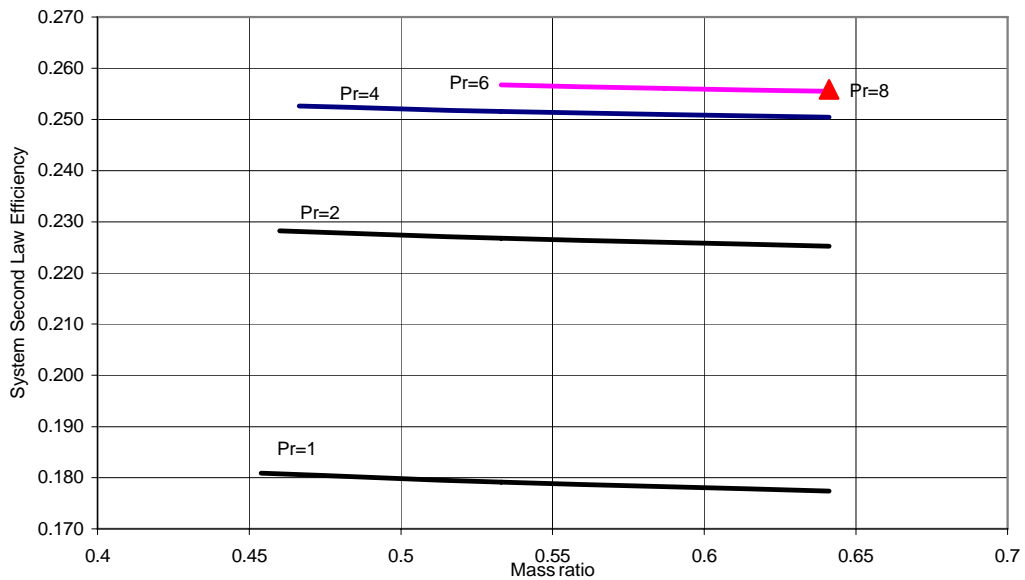


Figure 5. 12 : System second law efficiency vs mass ratio

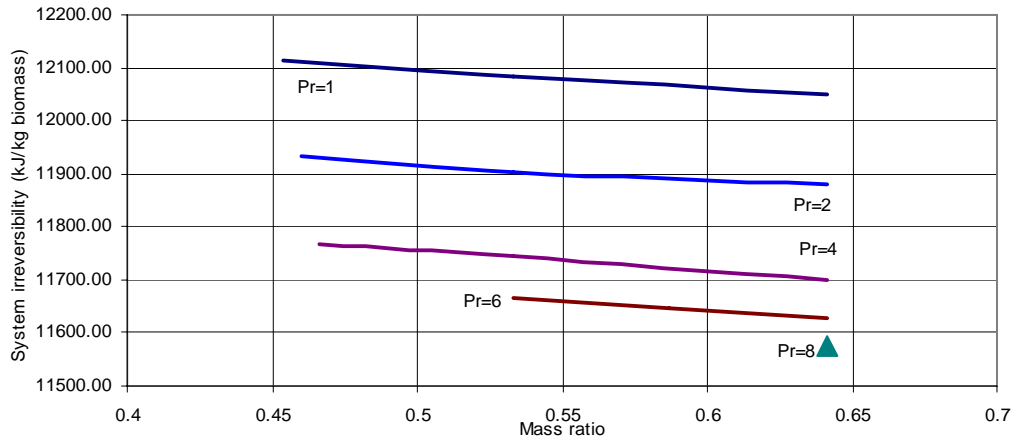


Figure 5. 13 : System total irreversibility vs mass ratio

When SOFC is considered, the maximum second law efficiency is at atmospheric pressure at System 2 and does not considerably change with mass ratio (Fig. 5.14). In Fig. 5.15, for SOFC irreversibility, minimum irreversibility is at System 2 as for the second law efficiency and the minimum is at $M_R=0.4539$. This point is the maximum work output point for System 2 as given in Fig. 5.7.

For the combustor and gasifier the irreversibility values for all cases are given in Fig. 5.16 and 5.17. Combustor irreversibility is maximum at $P_r=8$ and $M_R=0.6411$. The irreversibility increases with increasing mass and pressure ratio. This is because the heat exergy increases and exergy difference decreases with increasing mass and pressure ratio.

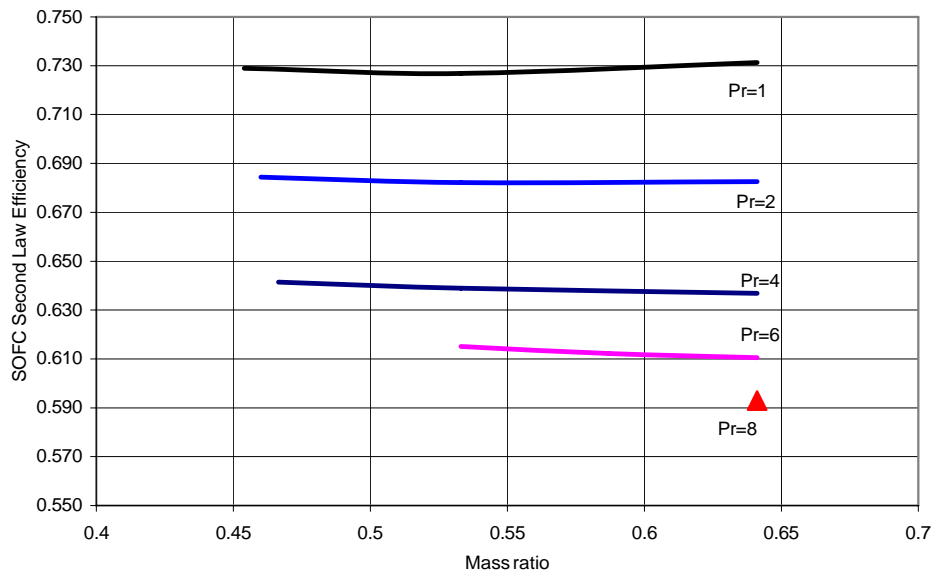


Figure 5. 14 : SOFC second law efficiency vs mass ratio

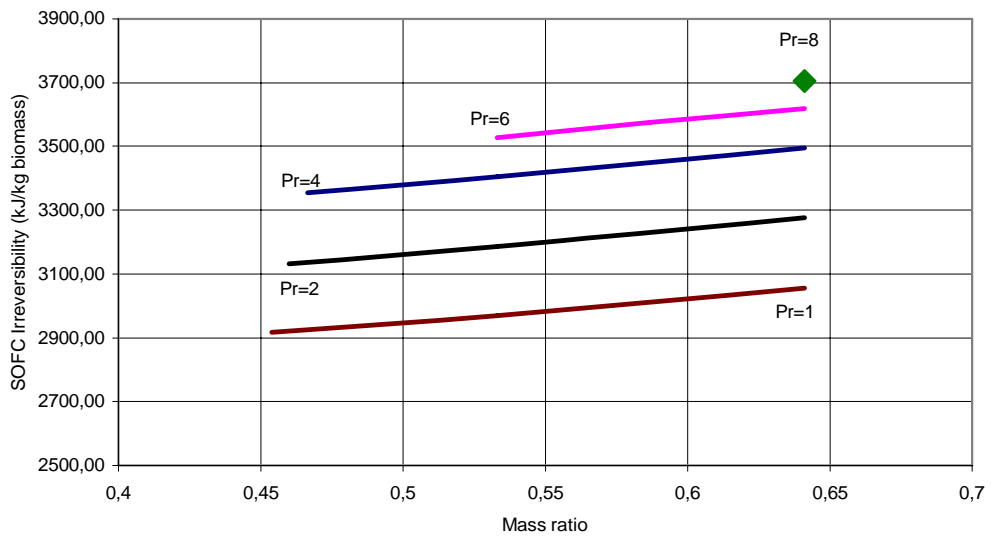


Figure 5. 15 : SOFC irreversibility vs mass ratio

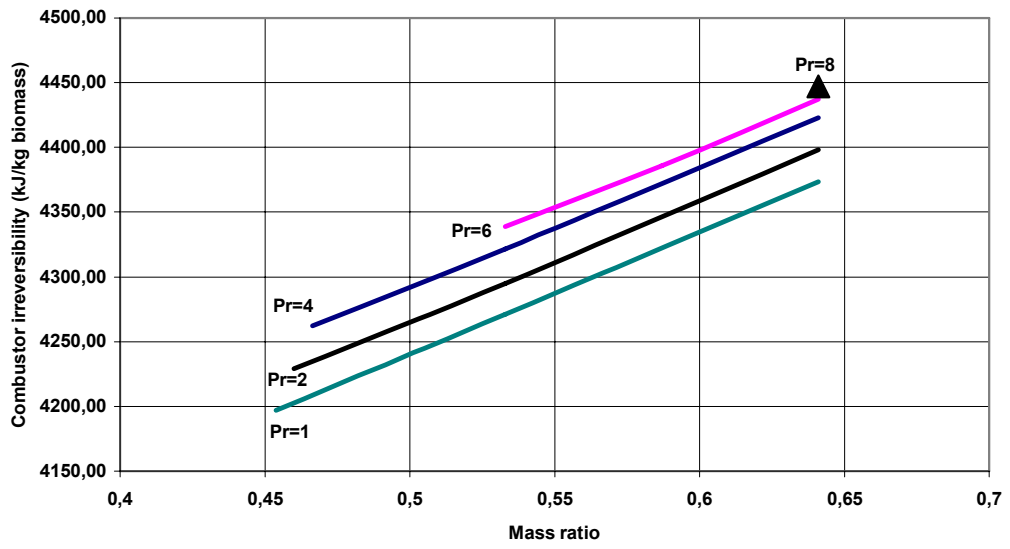


Figure 5. 16 : Combustor irreversibility vs mass ratio

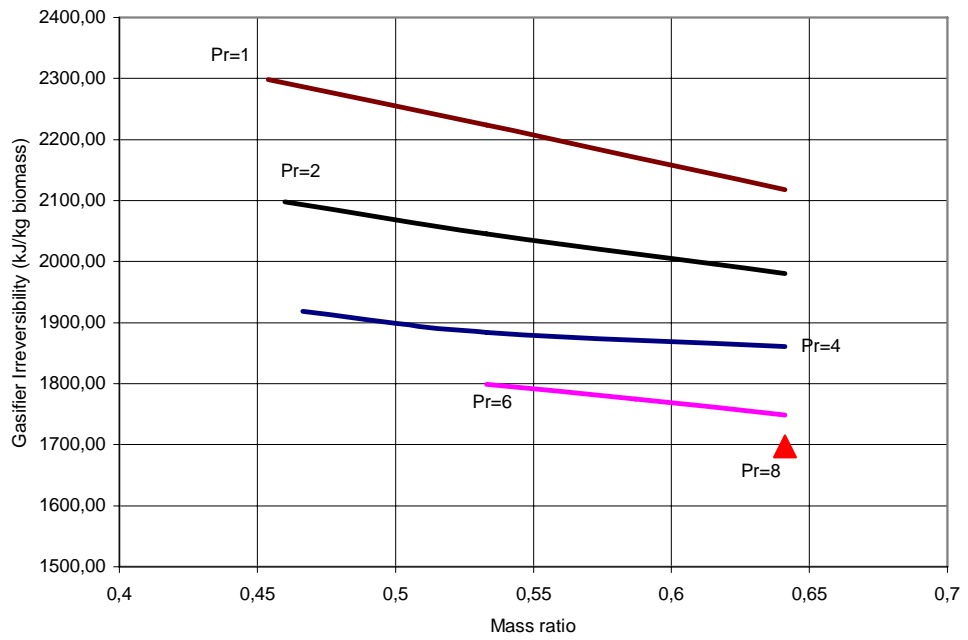


Figure 5. 17 : Gasifier irreversibility vs mass ratio

For gasifier, the maximum irreversibility is at atmospheric pressure at System 2 and $M_R = 0.4539$. As mass and pressure ratios increase, the irreversibility decreases. This is because the heat input exergy decreases and exergy difference between inlet and outlet increases with these increasing mass and pressure ratios because of same considerations of Fig. 5.11.

For the GT, the second law efficiency and irreversibility values can be seen in Fig. 5.18 and 5.19. There is no GT for System 2. Therefore, results have four pressure ratio lines changing from $M_R = 0.4665$ to $M_R = 0.6411$. Maximum second law efficiency occurs at $P_r=4$ and $M_R = 0.4665$. This point is the minima for irreversibility which explains the case for maximum power output, maximum second law efficiency and minimum irreversibility interaction.

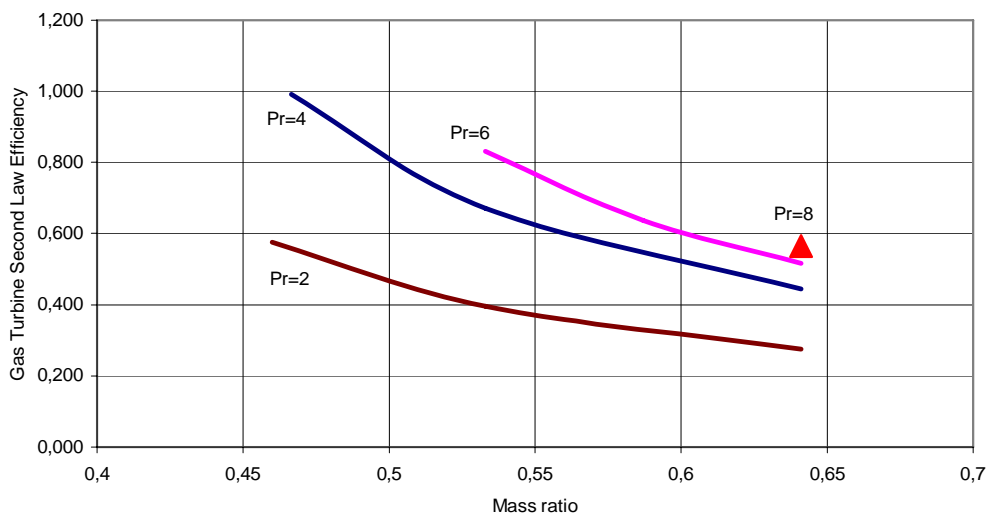


Figure 5. 18 : GT second law efficiency vs mass ratio

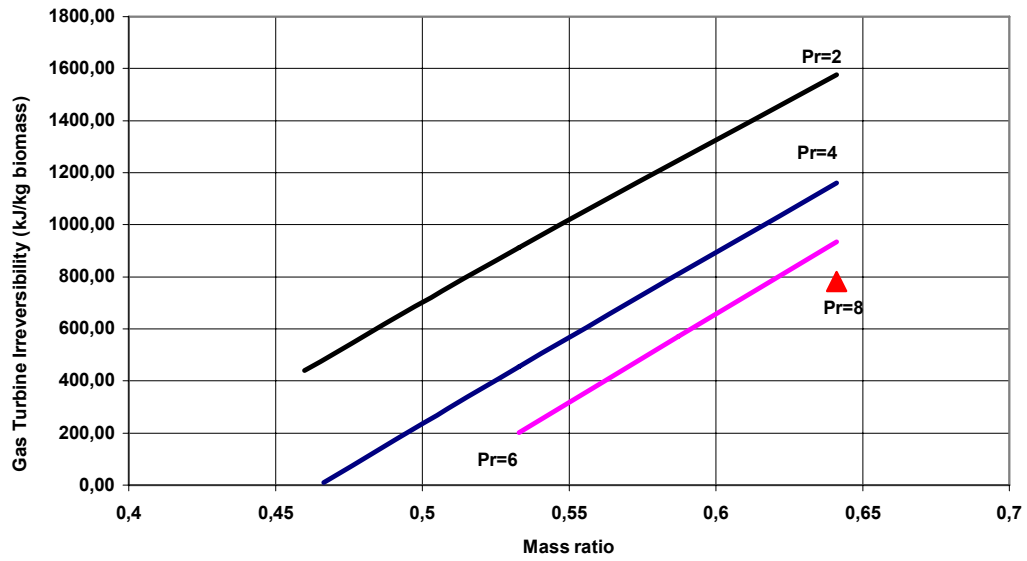


Figure 5. 19 : GT irreversibility vs mass ratio

As a result, the calculated enthalpy and exergy values for System 1 is given as an example for optimum operating point $M_R=0.6411$ and $P_T=8$ in Table 5.1.

Table 5. 1 : Energy, exergy and their normalized values for System 1 at $M_R=0.6411$ $P_T=8$

	<u>Energy</u>	<u>Normalized Energy</u>	<u>Exergy</u>	<u>Normalized Exergy</u>
<u>Work Output (kJ/kg biomass)</u>	3091.40	0.208*	3091.40	0.199*
<u>Heat Input (kJ/kg biomass)</u>	4173.42	0.281**	2586.70	0.167**
<u>Exhaust from System (kJ/kg biomass)</u>	11788.57	0.792*	813.38	0.053*
<u>Inlet Flow to System (kJ/kg biomass)</u>	10706.55	0.719**	12892.85	0.833**
<u>Irreversibility (kJ/kg biomass)</u>			11574.78	0.748***

* output from the system ** input to the system *** destructed in the system

5.3 Optimum Point For System

Hybrid system is a complex system and may work at many operating conditions. The parameters chosen for the hybrid system performance investigation were mass ratio, that is related to the air fraction of fuel cell and pressure ratio of the bottoming GT.

Optimum point for this study is the point where the system has its maximum power output among all operating points for same inlet fuel mass flow rate, same fuel utilization and same amount of inlet air.

The results for power output vs mass ratio were given in Fig. 5.5. To be able to see the optimum point among all cases, the power outputs should be redrawn vs pressure ratios.

The system power output values are given in Fig. 5.20 at different mass ratio values. The maximum power output point is at $P_r = 8$, $M_R = 0.6411$ at System 1. This point is the optimum operating point for the system for maximum power output.

For the electrical efficiency of the system Fig. 5.21 is given. The maximum electrical efficiency for the system is at the same point as the power output $P_r = 8$, $M_R = 0.6411$. System 2 efficiency value is far below System 1 values similar to the power output values in Fig. 5.20. Therefore, System 1 seems to be more efficient than System 2.

When we consider the fuel cell, the maximum power output is at $P_r = 8$, $M_R = 0.6411$ as given in Fig. 5.22. This figure shows that the performance of SOFC increases with increasing operating pressure for constant mass ratio. Maximum work output point for SOFC is also the optimum point for the system.

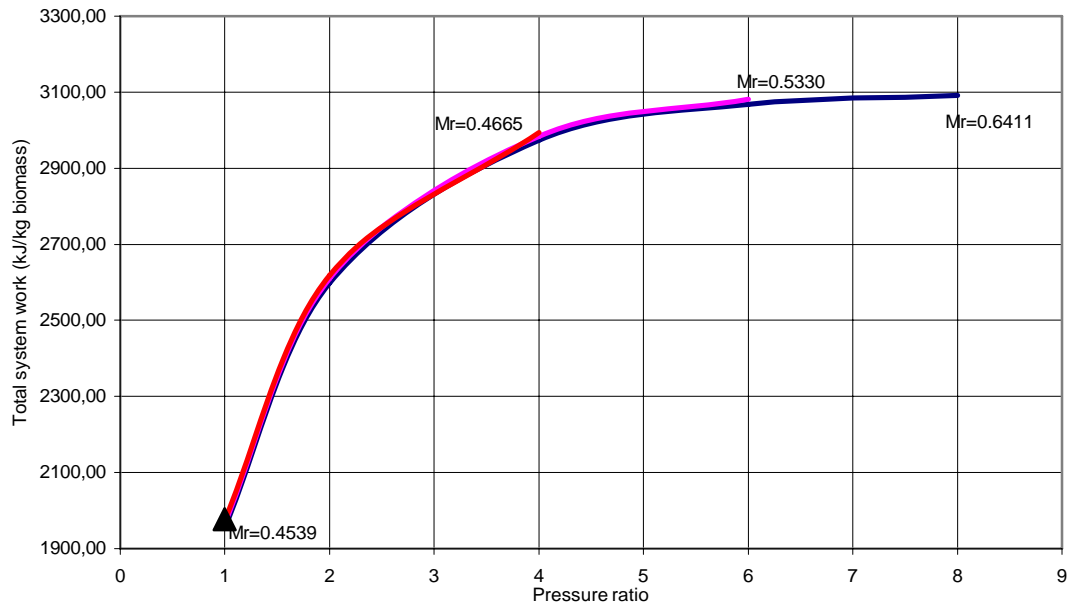


Figure 5. 20 : Total system power output vs pressure ratio

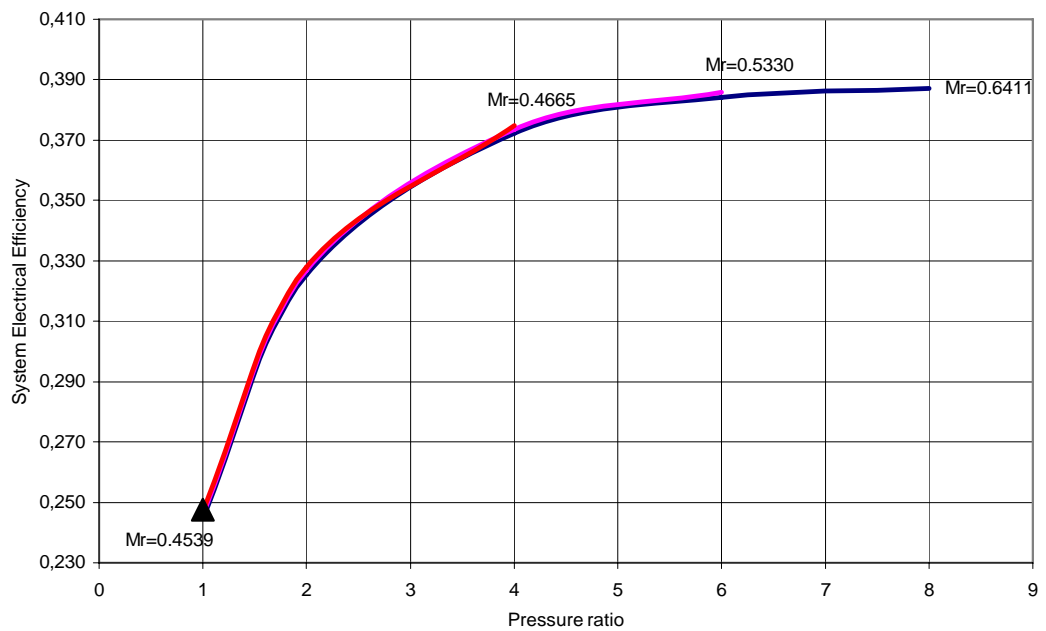


Figure 5. 21 : System electrical efficiency vs pressure ratio

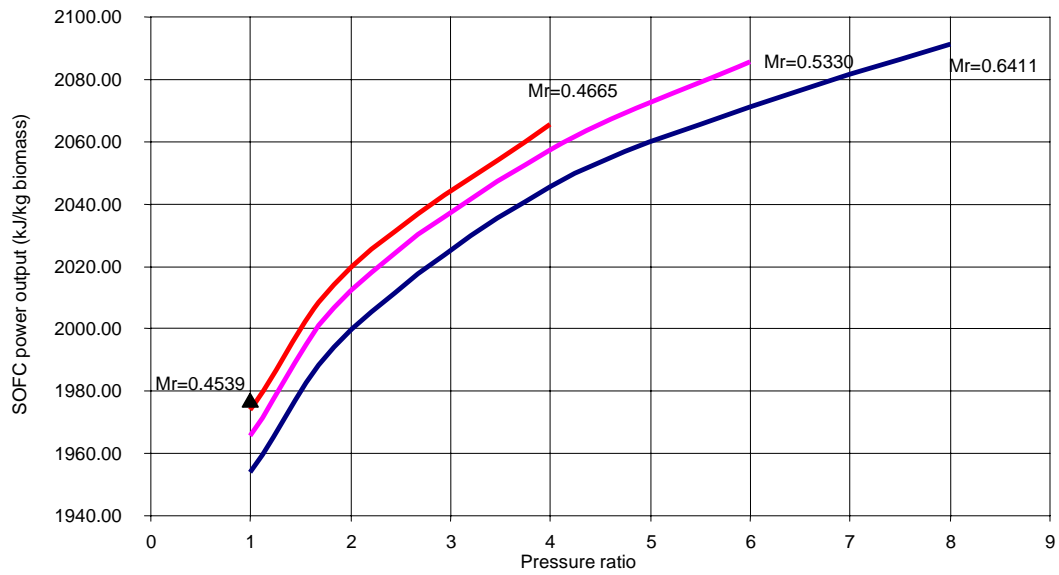


Figure 5. 22 : SOFC power output vs pressure ratio

Electrical efficiency of the fuel cell as given in Fig. 5.23 has the same characteristics as work output. The maximum electrical efficiency is at $P_r=8$, $M_R=0.6411$ which is the optimum point for system. It can be claimed that the maximum electrical efficiency for fuel cell at constant mass ratio occurs at maximum possible operating pressure for that mass ratio. The maximum electrical efficiency of SOFC at $M_R=0.6411$ is at maximum possible pressure ratio which is $P_r=8$.

The difference of total system work output and fuel cell work output originates from the GT. Since System 1 has an advantage of more power output because of having a GT, System 2 power output and efficiency values are lower. GT power output is given in Fig. 5.24. When Fig. 5.24 is investigated, the maximum power output can be seen at $P_r = 8$, $M_R=0.6411$ for System 1. This point is the optimum point for the system.

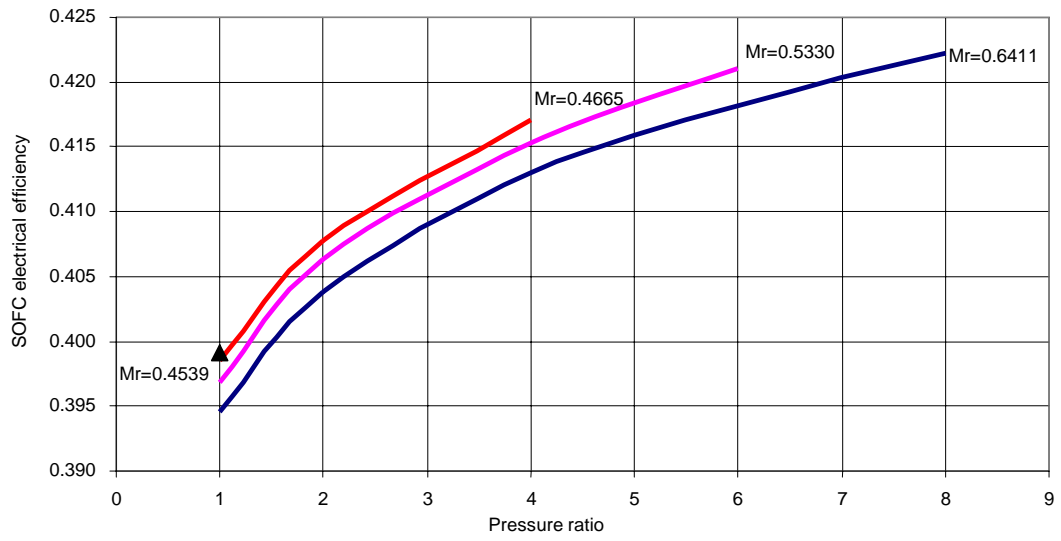


Figure 5. 23 : SOFC electrical efficiency vs pressure ratio

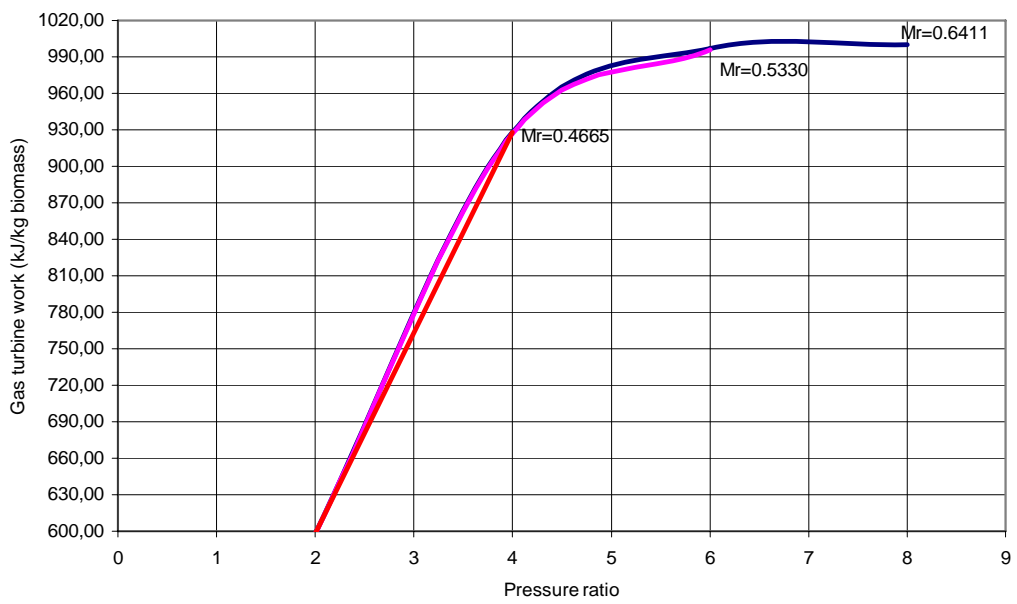


Figure 5. 24 : GT power output vs pressure ratio

Considering the total inlet heat transfer required for the system, the minimum point is at $P_r = 8$, $M_R = 0.6411$ as given in Fig. 5.25. The inlet heat transfer required for the system is an important parameter to investigate for both first and second law analysis. This minimum heat rate point is the optimum point for the system. Inlet enthalpy to the system does not change for cases, at optimum point the work output is maximum and outlet enthalpy is thus minimum.

System first law efficiency values can be seen in Fig. 5.26. The total inlet heat transfer and total power output values play important roles in this parameter. As the pressure ratio increases at constant mass ratio, the first law efficiency increases. This originates from the decreasing inlet heat transfer rate and increasing work output.

The required heat transfer values at different mass ratios are given for fuel cell, combustor and gasifier in Fig. 5.27, 5.28 and 5.29 respectively. As figures are investigated, for the SOFC, minimum heat transfer is required at atmospheric pressure at minimum mass ratio.

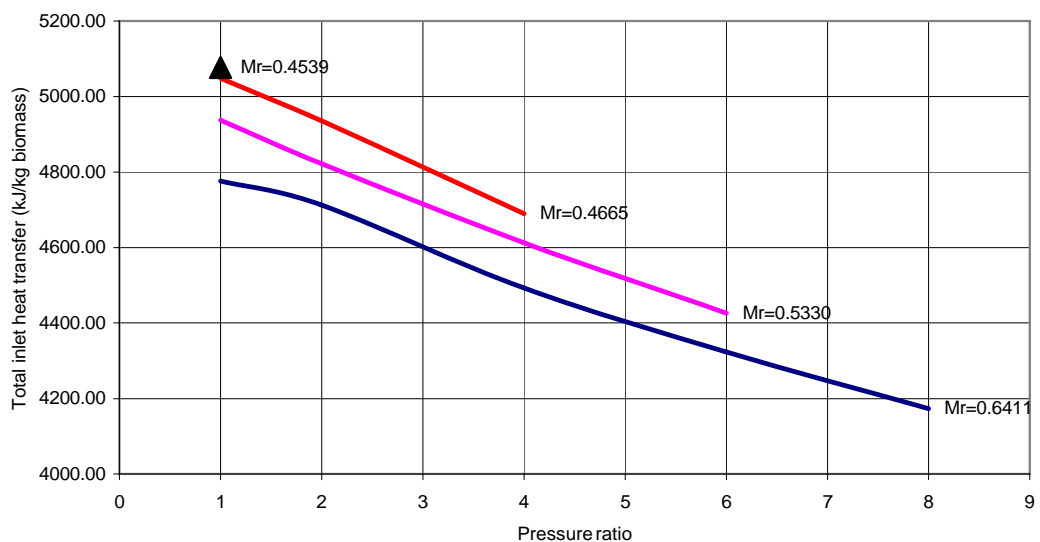


Figure 5. 25 : Total inlet heat transfer vs pressure ratio

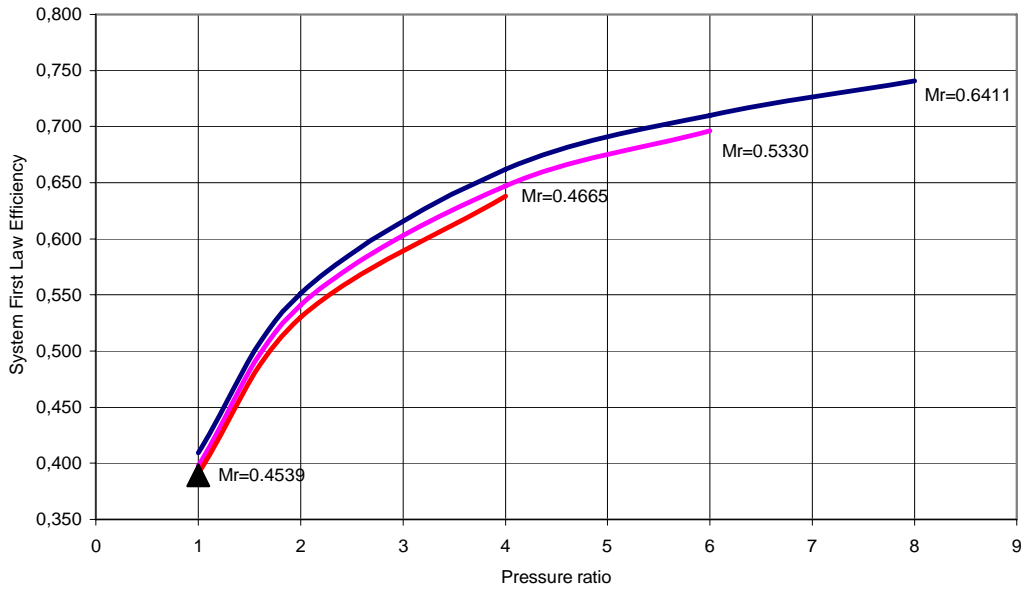


Figure 5. 26 : System first law efficiency vs pressure ratio

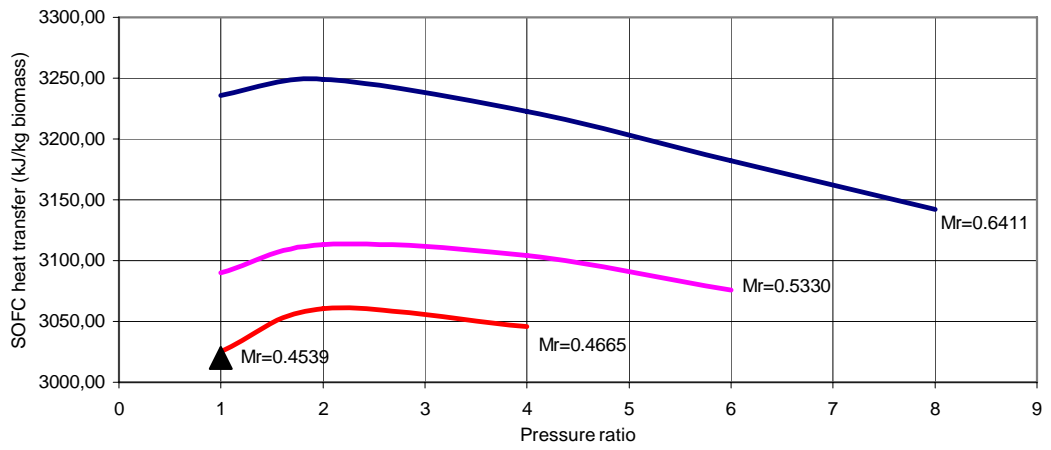


Figure 5. 27 : SOFC required heat transfer vs pressure ratio

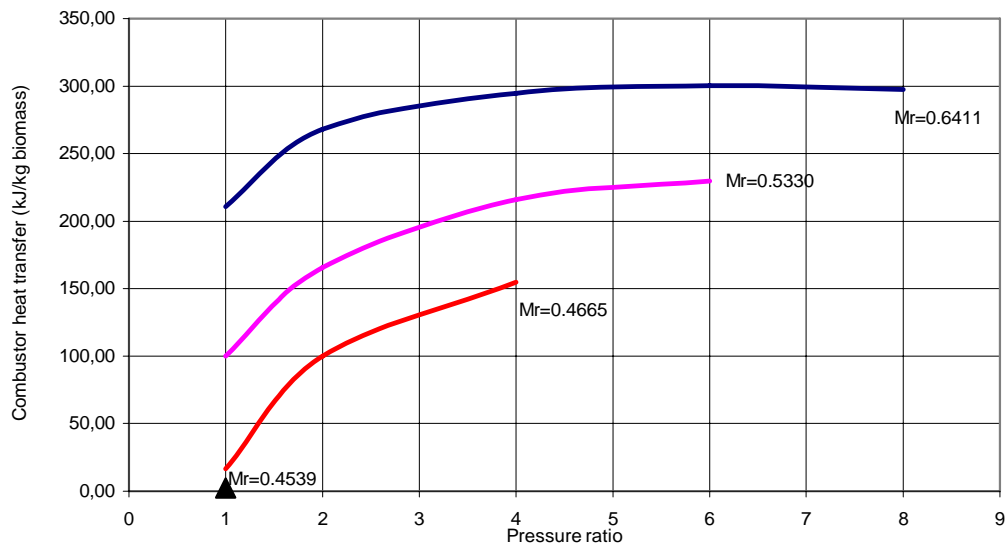


Figure 5. 28 : Combustor required heat transfer vs pressure ratio

For the combustor, the maximum required heat is at System 1 optimum point. As the pressure increases, the required heat transfer rate increases for the combustor.

Gasifier has its minimum heat transfer required at $P_r = 8$, $M_R = 0.6411$ at System1 which is the optimum point for system. As pressure increases at constant mass ratio, the required heat transfer decreases.

System second law efficiency values can be seen in Fig. 5.30. Maximum second law efficiency is at the optimum point for system as $P_r = 8$, $M_R = 0.6411$. Second law analyses then give the same optima for the system.

Since the inlet exergy is same for all cases, the irreversibility and power output values determine the outlet exergy from the system. Outlet exergy is related to the temperature of exhaust since the outlet mixture species amounts are the same for all cases. Having a low exhaust temperature shows minimum exergy outlet from the system. Exhaust temperature variation at different mass ratios of the system is given

in Fig. 5.31. The minimum value of exhaust temperature is at $P_r = 8$, $M_R = 0.6411$; at optimum point of the system which is expected.

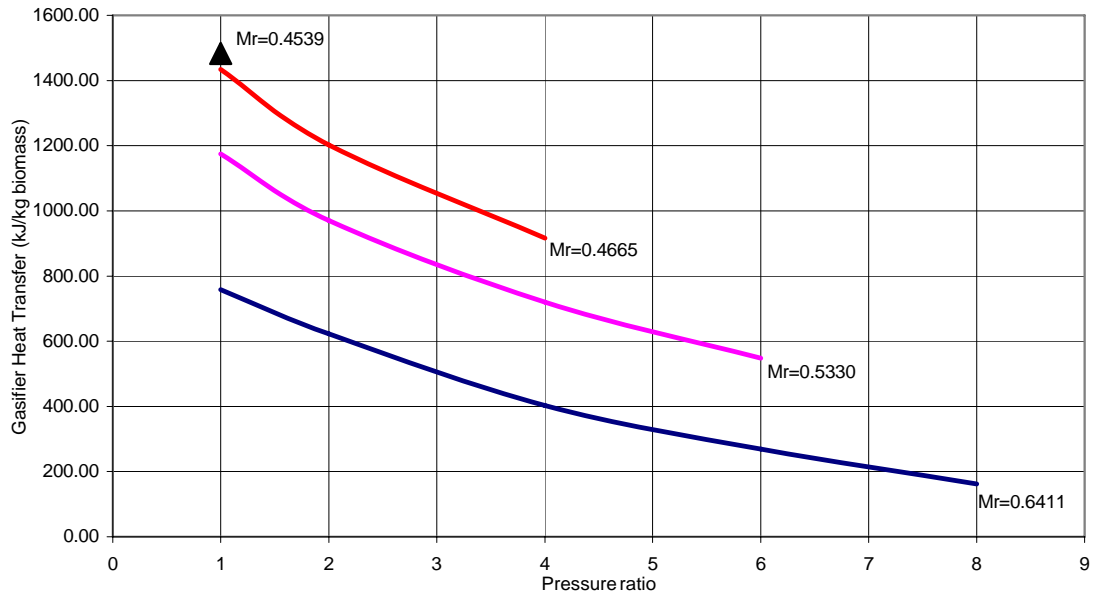


Figure 5.29 : Gasifier required heat transfer vs pressure ratio

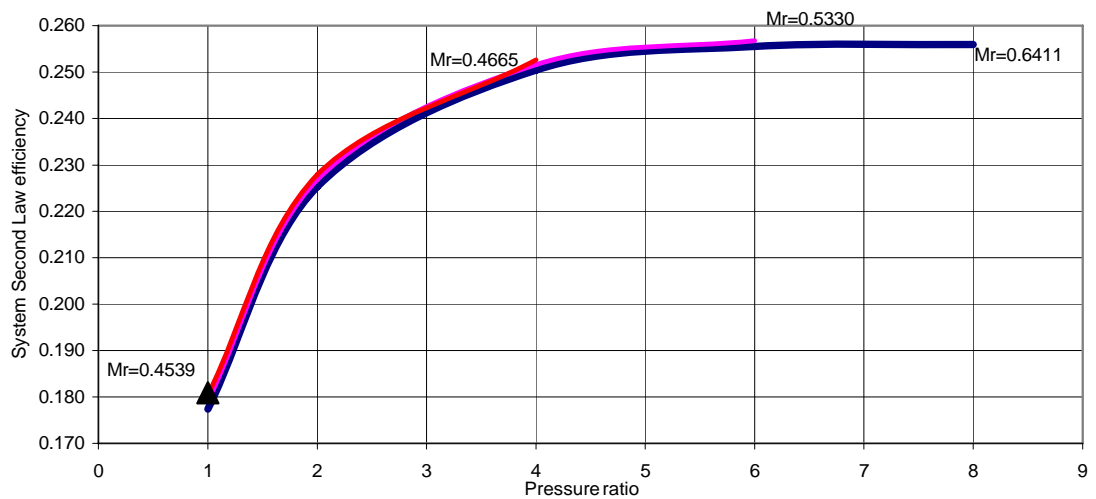


Figure 5.30 : System second law efficiency vs pressure ratio

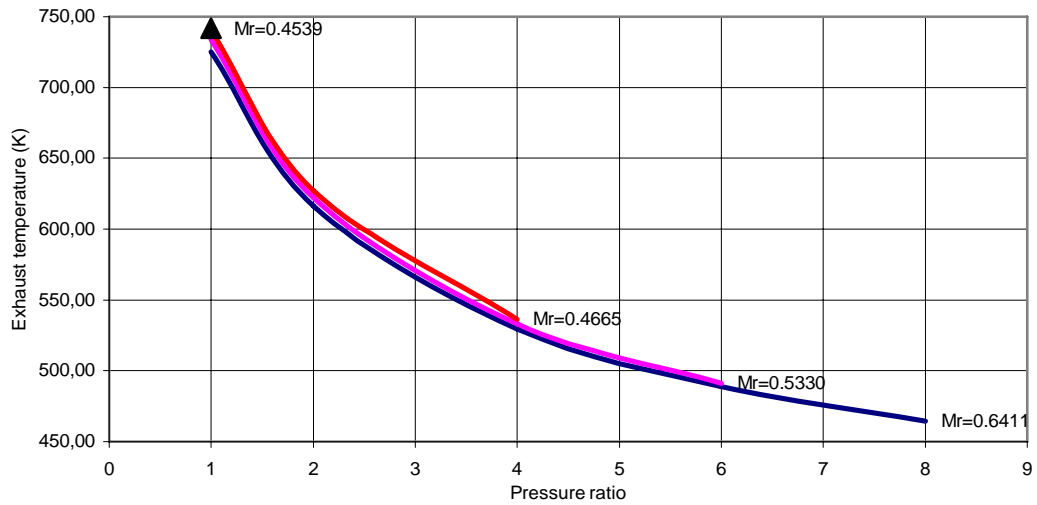


Figure 5. 31: Exhaust temperature vs pressure ratio

The irreversibility of total system can be seen in Fig. 5.32. For System 1, the irreversibility decreases with increasing pressure ratio. Utilizing the definition of second law efficiency in Equation 5.3, for high efficiency, the work should be at maximum and/or irreversibility should be minimum. The system irreversibility is minimum and work output is maximum at maximum second law efficiency point, which is the optimum point for the system.

When equipments are investigated separately, SOFC second law efficiency can be seen in Fig. 5.33. It shows that the maximum second law efficiency for fuel cell is at atmospheric pressure at System 2 at minimum mass ratio. At optimum point for system ($P_r = 8$, $M_R = 0.6411$), the fuel cell second law efficiency is minimum. As the pressure increases, exergy difference and work output increase and heat transfer exergy decreases. However, exergy difference increase is more than the increase in work output and decrease in heat transfer exergy. Therefore, the irreversibility decreases. This is the main reason for second law efficiency decrease of SOFC with increase in pressure.

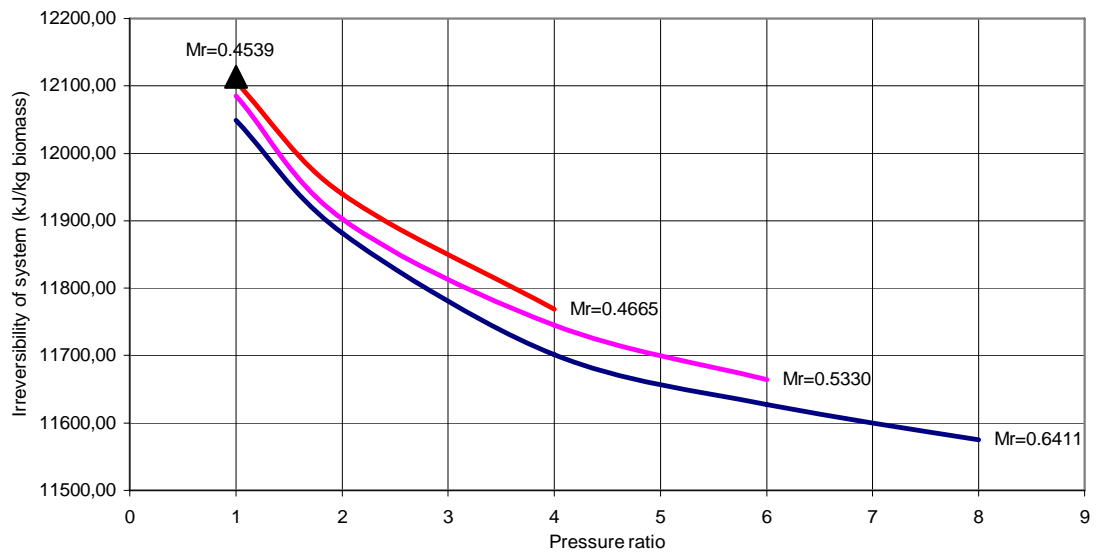


Figure 5. 32 : Irreversibility of the system vs pressure ratio

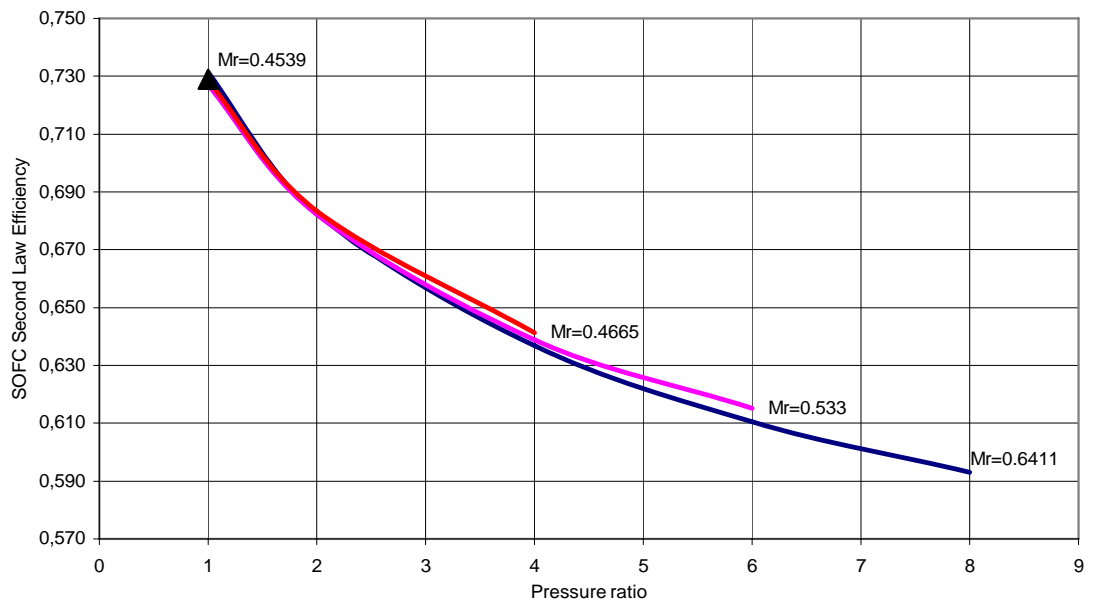


Figure 5. 33 : SOFC second law efficiency vs pressure ratio

The irreversibility for fuel cell is given in Fig. 5.34. The irreversibilities in SOFC are originated from reforming reaction, cracks, polarizations and incomplete reactions. In this study the polarization irreversibilities are constant because of constant polarization (constant current density) values. Main irreversibility reasons are chemical reactions taking place in SOFC. SOFC has its minimum irreversibility at its maximum second law efficiency point. The power output is minimum at this point. However, when the power output values are compared, it can be visualized that the difference is not so much. Therefore, irreversibility determines the second law efficiency variation at most. At optimum point of system ($P_r=8$, $M_R=0.6411$), the irreversibility of fuel cell is maximum.

For combustor, the irreversibility graph is given in Fig. 5.35. The maximum irreversibility of combustor is at $P_r=8$ at System 1 and minimum is at System 2. At optimum point of system ($P_r=8$, $M_R=0.6411$), the irreversibility is the maximum. Exergy difference and heat transfer exergy increases with increasing pressure so this is the main reason for increase in irreversibility.

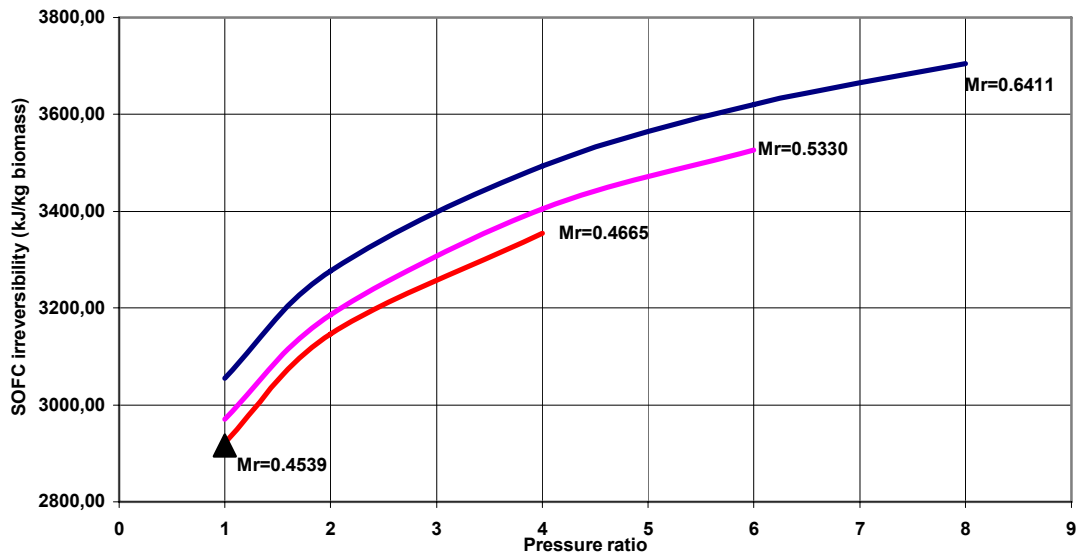


Figure 5. 34 : SOFC irreversibility vs pressure ratio

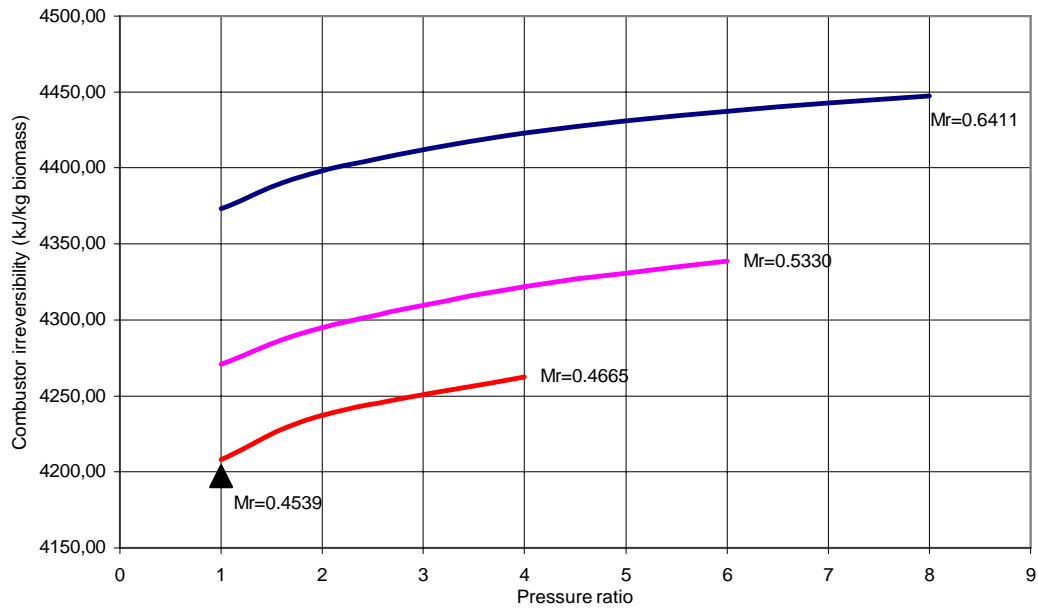


Figure 5. 35 : Combustor irreversibility vs pressure ratio

For gasifier, the irreversibility graph is given in Fig. 5.36. The minimum irreversibility value is at $P_r=8$, $M_R=0.6411$, the optimum point of the system. The maxima is at System 2. When the pressure ratio increases, the exergy difference for the gasifier increases but the heat transfer exergy decrease is more. Therefore, irreversibility decreases with increasing pressure ratio.

For the GT, the second law efficiency values are given in Fig. 5.37. The maximum second law efficiency is at $P_r=4$, $M_R=0.4665$. Since there is no GT in System 2, the results are given only for System 1 pressure ratio values. The maximum second law efficiency is related to the work output and irreversibility. The irreversibility for GT is in Fig. 5.38. The minimum irreversibility value is at maximum second law efficiency point of GT ($P_r=4$, $M_R=0.4665$). Since the work output does not change considerably with mass ratio for GT, irreversibility determines the gas turbine second law efficiency.

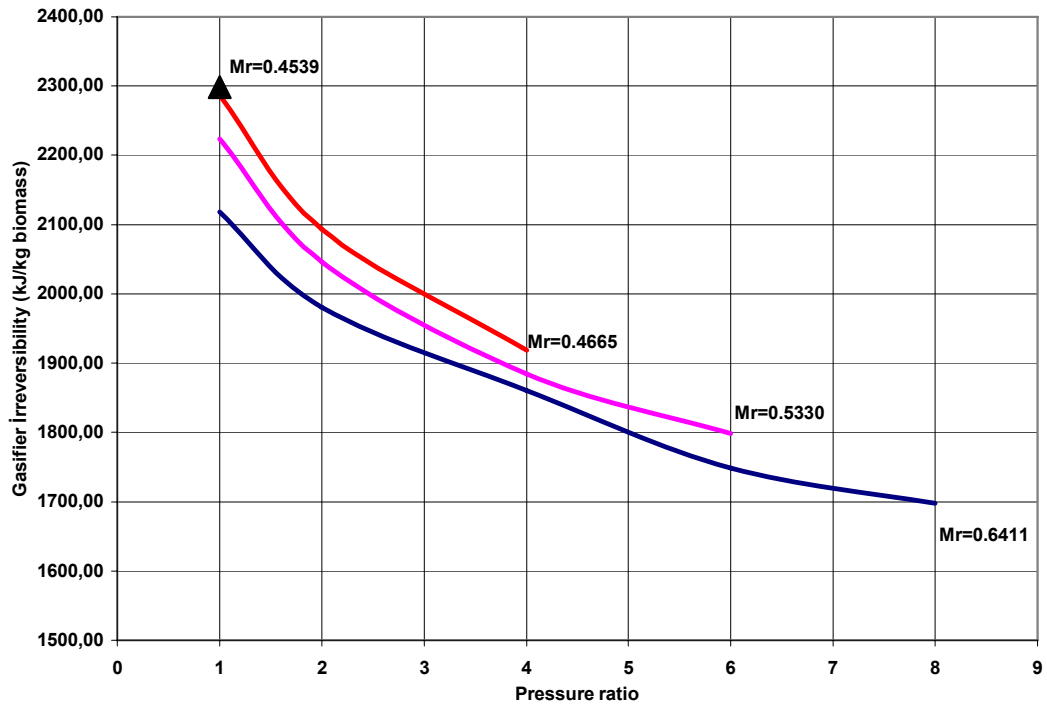


Figure 5. 36 : Gasifier irreversibility vs pressure ratio

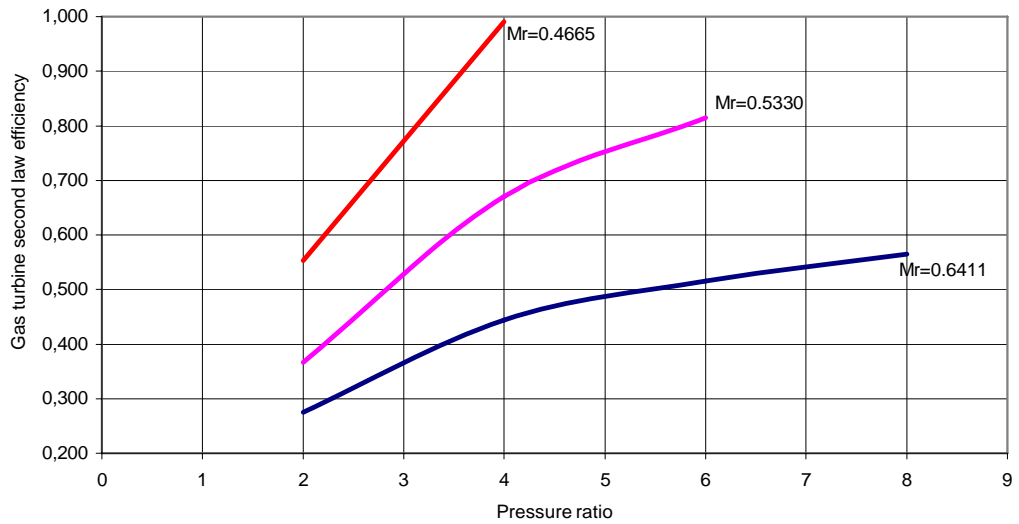


Figure 5. 37 : GT second law efficiency vs pressure ratio

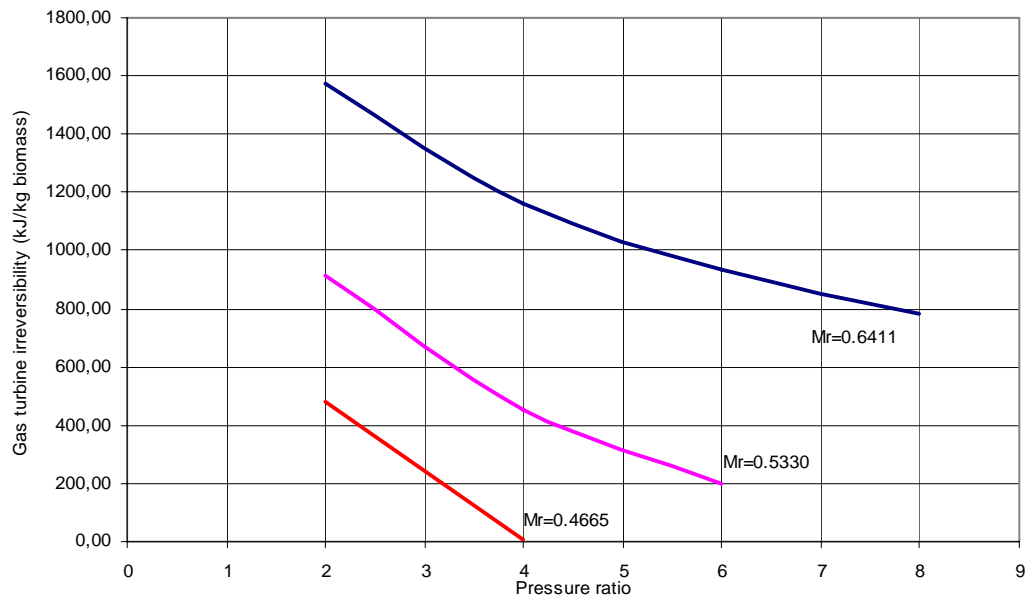


Figure 5. 38 : GT irreversibility vs pressure ratio

CHAPTER 6

CONCLUSION

System 1 in this study is a hybrid system consisting of a SOFC and a bottoming GT and System 2 is set without a GT. The first and second law analyses of all equipments with electrochemistry analyses of fuel cell are performed with a code written in MATLAB editor. The overall investigation of the system shows that the electrical efficiency is between 0.25-0.40 and first law efficiency is between 0.40-0.75. In literature, the system electrical and first law efficiency values vary between 0.20-0.80 [2, 8, 25, 26, 27]. The results may change according to the biomass type used and gasification results. The electrical efficiency definition term in Equation 5.2 may show either the producer gas LHV after gasification process as the fuel or the biomass LHV at the inlet of system. In this study it is taken to be the producer gas after gasification. The gasification results of literature are different since the operating conditions and types of gasifiers are different than this study. Gasification in this study is an air gasification while in literature steam gasification is mostly utilized. Also LHVs of literature studies fuel types are different. Mostly natural gas fed systems are investigated. Biomass fed systems have lower efficiencies because of gasification processes. If systems have more recuperators and compressors to have more efficient use of heat and pressure, the electrical efficiencies become higher [26]. All these parameters determine the difference on electrical efficiency of whole system. However, the values of this study are in acceptable range.

For the first and second law analysis results, the exhaust temperature shows the difference of the effect of the gas turbine in the system. In System 1, the exhaust temperatures are lower than System 2. This difference of exhaust temperatures of System 1 and System 2 may be compared by increasing the amount of hot water flow in System 2. Therefore, it can be said that System 1 has higher first law and electrical

efficiencies in terms of net work output. However, in terms of hot water gain, System 2 seems more efficient.

For SOFC, the electrical efficiency values in this study change between 0.39-0.43. The corresponding results in literature are between 0.50-0.75 for 50-85% fuel utilisation values mostly higher than that is used in this study as 60% [8, 15, 18, 25, 28, 29]. In electrical efficiency of fuel cell, fuel utilisation is an important factor. If in this study, the fuel utilisation would be higher like 85 %, the efficiency would be as 57 % (nearly 15 % more). The overpotentials are constant in all cases because fuel utilisation and fuel amount (reacted hydrogen, carbon monoxide and methane) are the same for all analyses cases. That means the operating current density is the same. Therefore, there is no difference in overpotentials of study cases. In literature the overpotentials are in the range 0.16- 0.35 V for fuel cell at 1073 K [1, 3, 30]. In this study the total overpotential is 0.202 V. The operating voltage values of this study are between 0.68-0.74 V and in literature they are between 0.65-0.75 V at same current density value of this study [3]. The values in this study are in acceptable ranges according to literature.

The second law efficiency of the system is between 0.16-0.26. There are not so many studies investigating the second law analyses of hybrid systems. However, there are results for SOFC second law efficiencies. In this study, SOFC second law efficiency varies between 0.59-0.73. These limits are not far away from the literature results being 0.50-0.73 for different fuel and reforming types and air amount for fuel cells [15, 18]. The values are in acceptable ranges.

For GT performance, the second law efficiency values in literature change between 10-80 % [1, 31, 32, 33]. For present study, the values are between 0.30-0.95. The difference originates from the fuel utilized and combustion integration into the GT. In this study the GT includes a heat exchanger instead of a combustor. The

combustor is outside the GT. The outlet of combustor enters the turbine however compressor outlet air enters the fuel cell instead of combustor.

The irreversibilities in the system originates mostly from the gasification, SOFC and combustion sections. That result shows the same inference as literature. This is unavoidable due to the irreversible nature of high temperature reactions far from chemical equilibrium like combustion and gasification [8]. The irreversibility of system decreases with increasing pressure ratio of the GT. For irreversibility of fuel cell, the condition is the opposite. Increase in pressure causes increase in irreversibility of the fuel cell.

The effect of increase of pressure on SOFC performance can also be seen at power and voltage output results. For higher operating pressures, fuel cell can produce more electrical power and operating voltages for same fuel amount and fuel utilisation. In literature, the same conclusion is valid [3, 8, 34, 35].

As the air amount entering the fuel cell increases, for constant fuel utilisation, the partial pressure of oxygen in the cathode decreases. This results in a lower operating voltage and thus lower power outputs for constant current density. In the literature, the plant and fuel cell efficiency increases with decreasing air amount at constant pressure line [34]. Therefore, the results found in this study are logical.

Increase in the mass ratio (air separated for fuel cell) decreases the air amount for the gasification for constant air inlet to the system. Using less air for gasification in this study decreases the heat required for the process and decreases the irreversibility at constant pressure. Therefore, increasing the mass ratio causes less losses in gasification. For low air amounts of gasification, the quality of producer gas (LHV of the gas) is higher [16]. Increase in pressure ratio causes decrease in gasifier irreversibility. Then, it should be noted that, lower air amounts (to have high quality producer gas) and pressurized conditions are suitable operating conditions for

gasifiers. In literature, for air gasification, air/fuel ratio is low for optimization and half of the producer gas is given to be N_2 as in this study [36]. The pressure is said to have a slight increasing effect on gasification efficiency [37]. Therefore, the results of this study seem valid.

The fuel type used in this study is hybrid poplar. It is a kind of biomass having a relatively high LHV. It is widely found and grown in Turkey, in coastal areas and off-the-coast areas up to 800-1000 meters height and around Middle and South-East Anatolia and can be harvested by 10-12 years [38]. The most important advantage of biomass is related to the greenhouse gas, CO_2 emission. When biomass is burnt, CO_2 is released. However, as it originates from harvested or processed plants, which have absorbed it from the atmosphere in the first place, no additional amounts are involved. However, it should be grown and utilized on a sustainable manner [39]. Therefore, it is a major feature for biomass to be chosen.

When biomass is compared to other types of fuels of hybrid systems, which are mainly natural gas, pure hydrogen or coal, gasification becomes important. Efficient gasification may result in more qualified producer gas, more chance of utilisation of fuel and higher LHV gas. If gasification is not effective and the biomass fuel cannot be converted efficiently into fuels of fuel cell (i.e H_2 , CO and CH_4), lower amounts of fuel for fuel cell will enter the cell and electrical output will be lower than expected. Using pure hydrogen is the most efficient and direct way to gain power from fuel cell. However, storage is a major problem for hydrogen. It is relatively high cost and problematic. Therefore, instead of producing hydrogen and store it as it is, natural gas or biomass type fuels are used in producing power to get rid of the high cost. They are naturally available storage ways for hydrogen with low or no cost.

Heat rate required for the total system operation decreases with increasing pressure ratio. Both fuel cell and gasifier heat rate requirements have the similar variations.

Therefore, total inlet heat transfer is decreasing with increasing pressure ratio. Similar tendencies exist in literature [35].

As the concluding remarks, System 1 as a hybrid system consisting of a SOFC and a bottoming GT is more advantageous than System 2 because of its higher power output and efficiency values. The reason is the GT effect on the system. It supplies more net output and increases the efficiency values. SOFC is an acceptable choice for the system because of its high operating temperature and less sensitivity to CO when compared to other kinds of fuel cells. This ability allows fuel cell to use different kinds of biomasses. Pressure and air effects on the fuel cell and other items may be observed throughout the study. The results of this study shows that pressure increases the performance of fuel cell and the system.

The present study is for first and second law analyses of a hybrid system. In future, the study may be improved in order to decrease the irreversibility and increase the total power output and the efficiencies of each of the equipments and the overall system. Different kinds of biomass or different solutions for gasification may be studied in order to achieve this remark.

REFERENCES

1. Hideyuki Uechi, Shinji Kimijima, Nobuhide Kasagi, “*Cycle Analysis of Gas Turbine–Fuel Cell Cycle Hybrid Micro Generation System*”, *Journal of Engineering for Gas Turbines and Power*, vol. 126, pp 755-762, October 2004.
2. A. F. Massardo, C. F. McDonald, T. Korakianitis, “*Micro turbine/Fuel Cell Coupling for High Efficiency Electrical-Power Generation*”, *Journal of Engineering for Gas Turbines and Power*, vol. 124, pp 110-116, January 2002.
3. Joshua E. Freeh, Joseph W. Pratt, Jacob Brouwer, “*Development of a Solid Oxide Fuel Cell/Gas Turbine Hybrid System Model for Aerospace Applications*”, *Proceedings of ASME Turbo Expo 2004, Power for Land, Sea, Air, Vienna, Austria, June 2004*.
4. J. Szargut, D.R. Morris, F.R. Steward, “*Exergy Analysis of Thermal, Chemical and Metallurgical Processes*”, Hemisphere, New York, 1988.
5. Peter McKendry, “*Energy Production from Biomass (part 3) : Gasification Technologies*”, *Bioresource Technology*, vol. 83, pp 55-63, 2002.
6. Kevin R. Craig, Margaret K. Mann, “*Cost and Performance Analysis of Biomass-Based Integrated Gasification Combined-Cycle (BIGCC) Power Systems*”, *National Renewable Energy Laboratory, Colorado, October 1996*.

7. G. Chen, H. Spliethoff, J. Andries, M. P. Glazer, “*Biomass Gasification in a Circulating Fluidized Bed-Part 1 : Preliminary Experiments and Modelling Development*”, *Energy Sources*, vol. 26, pp 485-498, 2004.
8. Tobias Proell, Reinhard Rauch, Christian Aichernig, Hermann Hofbauer, “*Coupling of Biomass Steam Gasification and an SOFC-Gas Turbine Hybrid System for Highly Efficient Electricity Generation*”, *Proceedings of ASME Turbo Expo 2004, Power for Land, Sea, Air, Vienna, Austria, June 2004*.
9. Leong Poon, “*Literature Review on the Contribution of Fire Resistant Timber Construction to Heat Release Rate*”, *Warrington Fire Research* , version 2b, Australia.
10. Mark Jan Prins, “*Thermodynamic Analysis of Biomass Gasification and Torrefaction*”, *Eindhoven University of Technology, Netherlands, 2005*.
11. Krister Stahl, Magnus Neergaard, “*IGCC Power Plant for Biomass Utilisation Varnamo, Sweden*”, *Biomass and Bioenergy*, vol. 15, pp 205-211, 1998.
12. C. Z. Wu, H. Huang, S. P. Zheng, X. L. Yin, “*An Economic Analysis of Biomass Gasification and Power Generation in China*”, *Bioresource Technology*, vol. 83, pp 65-70, 2002.
13. Global Climate and Energy Project (GCEP), “*An Assessment of Biomass Feedstock and Conversion Research Opportunities*”, *Stanford University, Spring 2005*.

14. Adam Wojcik, Hugh Middleton, Ioannis Damopoulos, Jan Van Herle, “*Ammonia As a Fuel in Solid Oxide Fuel Cells*”, *Journal of Power Sources*, vol. 118, pp 342-348, 2003.
15. Kai W. Bedringas, Ivas S. Ertesvag, Stale Byggstoyl, Bjorn F. Magnussen, “*Exergy Analysis of Solid-Oxide Fuel Cell (SOFC) Systems*”, *Energy*, vol.22, pp 403-412, 1997.
16. Andrea Corti, Lidia Lombardi, “*Biomass Integrated Gasification Combined Cycle with Reduced CO₂ Emissions: Performance Analysis and Life Cycle Assessment (LCA)*”, *Energy*, vol. 29, pp 2109-2124, 2004.
17. Florian Zink, Yixin Lu, Laura Schaefer, “*A Solid Oxide Fuel Cell System for Buildings*”, *Energy Conversion and Management*, vol. 48, pp 809-818, 2007.
18. S. H. Chan, C. F. Low, O. L. Ding, “*Energy and Exergy Analysis of Simple Solid-Oxide Fuel-Cell Power Systems*”, *Journal of Power Sources*, vol. 103, pp 188-200, 2002.
19. Kouros Sedghisigarchi, Ali Feliachi, “*Dynamic and Transient Analysis of Power Distribution Systems with Fuel Cells-Part 1: Fuel-Cell Dynamic Model*”, *IEEE Transactions on Energy Conversion*, vol. 19, pp 423-428, June 2004.
20. Matthew M. Mench, Chao-Yang Wang, Stefan T. Thynell, “*An Introduction to Fuel Cells and Related Transport Phenomena*”, Electrochemical Engine Center, The Pennsylvania State University, USA.
21. Frank P. Incropera, David P. De Witt, “*Fundamentals of Heat and Mass Transfer (Fourth Edition)*”, John Wiley & Sons, 1996.

22. http://www.deschamps.com/products/product_detail.php?application_ID=8&product_ID=60 (October 15, 2008).
23. <http://www.boschevaletleri.com/?5=RDG8012TR> (September 13, 2008).
24. <http://www.wwf.org.tr/wwf-turkiye-hakkinda/ne-yapiyoruz/su-kaynaklari/> (August 2008).
25. A. O. Omosun, A. Bauen, N. P. Brandon, C. S. Adjiman, D. Hart, “*Modelling System Efficiencies of Two Biomass-Fuelled SOFC Systems*”, Journal of Power Sources, vol. 131, pp 96-106, 2004.
26. S. H. Chan, H. K. Ho, Y. Tian, “*Modelling of Simple Hybrid Solid Oxide Fuel Cell and Gas Turbine Power Plant*”, Journal of Power Sources, vol. 109, pp 111-120, 2002.
27. S. E. Veyo, L. A. Shockling, J. T. Dederer, J. E. Gillett, W. L. Lundberg, “*Tubular Solid Oxide Fuel Cell/gas Turbine Hybrid Cycle Power Systems: Status*”, Journal of Engineering for Gas Turbines and Power, vol. 124, pp 845-849, 2002.
28. Christoph Stiller, “*Design Operation and Control Modelling of SOFC/GT Hybrid Systems*”, Norwegian University of Science and Technology, March 2006.
29. E. Bilgen, “*Exergetic and Engineering Analyses of Gas Turbine Based Cogeneration Systems*”, Energy, vol. 25, pp 1215-1229, 2000.
30. http://www.fuelcellknowledge.org/research_and_analysis/cell_performance/index.html (September 13, 2008).

31. George T. Lee, Frederick A. Sudhoff, "*Fuel Cell/Gas Turbine System Performance Studies*", Fuel Cells '96 Review Meeting, Morgantown, West Virginia, August 1996.
32. N. Lymberopoulos, "*Micro turbines and Their Application in Bio-Energy*", Centre of Renewable Energy Sources (C.R.E.S), Greece, January 2004.
33. Y-C Huang, C-I Hung, C-K Chen, "*Exergy Analysis for a Combined System of Steam-Injected Gas Turbine Cogeneration and Multiple-Effect Evaporation*", Proceedings of the Institution of Mechanical Engineers, vol. 214, Part A, Power and Energy, 2000.
34. A. F. Massardo, F. Lubelli, "*Internal Reforming Solid Oxide Fuel Cell-Gas Turbine Combined Cycles (IRSOFC-GT): Part A- Cell Model and Cycle Thermodynamic Analysis*", Journal of Engineering for Gas Turbines and Power, vol. 122, pp 27-35, January 2000.
35. S. Ghosh, S. De, "*Energy Analysis of a Cogeneration Plant Using Coal Gasification and Solid Oxide Fuel Cell*", Energy, vol. 31, pp 345-363, 2006.
36. Ayhan Demirbaş, "*Biomass Gasification for Power Generation in Turkey*", Energy Sources, Part A, vol. 28, pp 433-445, 2006.
37. Philippe Mathieu, Raphael Dubuisson, "*Performance Analysis of a Biomass Gasifier*", Energy Conversion and Management, vol. 43, pp 1291-1299, 2002.
38. <http://www.kavak.gov.tr/kavakcilik/mkvagtek/mkvagtek.htm> (August 22, 2008).

39. Ayhan Demirbaş, “*Biomass Resource Facilities and Biomass Conversion Processing for Fuels and Chemicals*”, *Energy Conversion and Management*, vol. 42, pp 1357-1378, 2001.